Antisense inhibition of *accA* suppressed *luxS* expression that is essential for quorum sense signaling, biofilm formation, and virulence

Tatiana Hillman[1]
[1]Biotechnology, TheLAB, Inc., Los Angeles, California, United States
Corresponding author: Tatianna Hillman[1]
E-mail: thillman@usc.edu & tatiana@thelabtech.net

ABSTRACT

Bacterial multiple drug resistance (MDR) is a major issue for the medical community. Gram-negative bacteria (GNB) exhibit higher rates of multidrug resistance. Gram-negative bacteria are more resistant to multiple antibiotics. The double membrane contains an outer membrane with a lipid bilayer of lipopolysaccharides (LPS) and an inner cytoplasmic membrane (IM). Gram-negative bacteria limit hydrophobic particle influx via OM and hydrophilic molecule import through the IM. The translation of *accA* produces the AccA subunits of acetyl-CoA carboxylase transferase (ACCase-CT) enzymes required for catalyzing the output of fatty acids (FA) and phospholipids of the IM. Inhibiting *accA* can eliminate the AccA subunits of the ACCase-CT enzyme, which then block and decrease FAS. A deletion of *luxS,* in which LuxS develops virulent biofilm via the LuxS/AI-2 QS system, also reduces the output of FAs. Because *accA* and *luxS* both affect the output of FAs, a possible link between *accA* and *luxS* was examined by antisense RNA inhibition of *accA* and then applying real-time PCR (qPCR) for absolute quantification of *luxS*. The gene *accA* was inhibited with antisense RNA and produced a qPCR product of 63 ng/µL. The inhibition of *accA* suppressed the expression of *luxS* to 199 qPCR products versus $1x10^6$ gene copies for the control. Bacterial cells that expressed antisense inhibition of *accA* also displayed a higher level of antibiotic susceptibility. Utilizing *accA* and *luxS* inhibitors to restrain FAS may provide potential targets for developing novel antimicrobial gene therapies for MDR-GNB.

Keywords: Antibiotic Resistance, Antibiotics, Biofilm, Carboxylase Enzymes, Autoinducers, Quorum Sensing, Antisense RNA, and Fatty Acid Synthesis

INTRODUCTION

Multiple drug resistant (MDR) bacteria present an enormous challenge for many medical communities and organizations, globally. For example, *A. baumanii* is an MDR-gram-negative bacterium that inhabits hospitals. *A. baumanii* bacteria cause 64% of urinary tract infections during the use of catheters [1]. Multiple drug resistance occurs when one bacterium is resistant to more than one antibiotic. Gram-negative bacteria produce a majority of multiple drug resistant bacterial infections. The cell envelope of gram-negative bacteria plays a prominent role in antibiotic resistance. The cell envelope of gram-negative bacteria consists of a phospholipid inner membrane (IM), a periplasmic space of peptidoglycan, and an outer membrane (OM). The cell envelope contains an inner membrane IM containing a phospholipid bilayer and an OM with a lipopolysaccharide region termed the LPS.

Due to this double membrane, gram-negative bacteria are partially protected from diffusible hydrophobic and hydrophilic compounds. LPS blocks the influx of hydrophobic molecules, and the IM phospholipid bilayer limits the internal transport of hydrophilic molecules. The structure of the double membrane for gram-negative bacteria causes antibiotic drug discovery to become an arduous task [2]. The double layer limits the accrual of antibiotics and enzyme inhibitors into the gram-negative bacterial cell. The membrane is a strong barrier in which antibiotics must break to access the intracellular region of bacterial cells. The membrane also creates concentration and electrical gradients between bacteria and its outer environment. The gradients are removed and detached when the cell membrane is damaged [3].

The OM of gram-negative bacteria contains a lipid bilayer, glycoproteins, and membrane proteins. The OM has a lipid bilayer, but it is not a bilayer composed of phospholipids [4]. The outer surface of the OM comprises glycolipids of LPS that can cause endotoxic shock during Gram-negative bacterial infection and septicemia. The two types of proteins located in the OM are lipoproteins, such as transmembrane proteins and β-barrel proteins known as porins [4]. Porins facilitate the influx of hydrophilic molecules, to pass through the OM. Lipoproteins are synthesized in the cytoplasm, transported to the IM, matured in the periplasmic space, fastened into the OM, and then anchored into the IM [5].

The IM of gram-negative bacteria is composed of a phospholipid bilayer, and the phospholipid (PL) bilayer is produced by the fatty acid type II synthesis pathway (FASII) [2]. The first phase of FASII includes the carboxylation of acetyl-CoA, which forms malonyl-CoA through a biotin carboxylase carrier protein (BCCP) and the acetyl-CoA carboxylase transferase (CT) enzyme. To begin the process of FASII, a change from malonyl-CoA into malonyl-ACP is required. Malonyl-ACP combines with acetyl-CoA to generate ketoacyl-ACP via the 3-oxoacyl-[acyl-carrier protein] synthase 3 (FabH). After FASII is initiated and completed, two carbons are added per cycle of fatty acid elongation that includes the

conversion of malonyl-ACP into acyl-ACP. Acetyl-CoA combines with a carboxyl group to form malonyl-CoA in an ATP-dependent reaction [7]. Bacterial fatty acid synthesis produces phospholipids required to stabilize and form plasma membranes.

The acetyl-CoA carboxylase complex is an essential enzyme for the first-rate limiting step in FAS of phospholipids. CT catalyzes the elongation of fatty acids. The gene *accA* encodes the AccA domain of the CT subunit. The ACCase enzyme has three subunits that include a biotin carboxylase (BC), biotin carboxyl carrier protein (BCCP), and an α2β2heterotetrameric carboxyltransferase (CT) [7]. The *accB* codes for BCCP and BC are translated from *accC*. The *accB* and *accC* (*accBC*) are transcribed simultaneously by the *accBC* mini operon [21]. The genes *accA* and *accD* encode the α-subunits and β-subunits, respectively. The α-subunit (*accA*) and β-subunit (*accD*) make up the CT portion of ACCase. Bacterial cells use enzymes that lyse glucose molecules into pyruvates. The ACCase complex subunit, termed AccA, transfers a carboxyl delivered through BC-BCCP to CT. The BC-BCCP positions a carboxyl from a pyruvate to the CT. The CT orients the carboxyl to acetyl-CoA that forms a malonyl-CoA.

Bacterial FAS can also significantly impact the production of biofilm and antibiotic susceptibility. A biofilm includes tight junctional communities of bacterial cells that have an extracellular matrix type of outer covering [8]. The cover of the extracellular matrix allows bacteria to attach to a biotic or abiotic surface. This extracellular matrix protects bacterial cells from external and environmental pressures. Yao and Rock confirmed the significant connection between biofilm formation and fatty acid synthesis enzymes contained in the structure of *S. aureus* [9]. More research is needed to further elucidate the link between the phospholipid membrane and the condition of a biofilm [10]. The metabolic fluxes that affect bacterial biofilm formation are not fully understood [8]. The link between bacterial metabolism and virulence needs further elucidation. For this reason and in this study, *accA* genes were silenced to disrupt FAS to examine the link between bacterial FA metabolism and biofilm, a major virulent factor.

accA was suppressed with interfering antisense RNAs (asRNAs) (Fig 1), and then its gene expression was quantified via real-time PCR (qPCR). The asRNAs were bound to sequences flanking the ribosome binding site and the start codon for the 150-base pair (bp) *accA* target mRNAs. The antisense RNA blocks ribosomal detection through the ribosomal binding site (RBS) and inhibits translation [11]. D-Glucose was also added to positive asRNA *accA* ((+)asRNA-accA) expressing *E.coli* cultures to affirm the interaction between the catabolism of glucose into carboxyls and *accA* gene expression. The (+)asRNA-*accA E.coli* cells enhanced with glucose molecules were then prepared for RNA isolation to perform qPCR of accA (qPCR-accA). accA encodes the AccA subunit of the acetyl-CoA carboxylase transferase enzyme (CT), so by using antisense RNA transcripts to inhibit *accA,* the CT enzyme lacked the AccA subunit needed for FA catalysis and production. Inhibiting *accA* with

asRNA transcripts interrupts the activation of FA synthesis, where less production of FAs may negatively distort the composition of the cell membrane lipid bilayers, which can increase the influx of antibiotics across the OM and IM.

.

LuxS affects biofilm composition and formation. LuxS, an autoinducer-2 (AI-2) producing S-ribosyl homocysteine lyase protein, mediates the production of AI-2 using 4,5,-dihydroxy-2,3-pentadione (DPD) as a precursor. Microarray analysis exposed five operons in a mutant ΔluxS strain of *Pneumococcal* bacteria. These five operons code for proteins responsible for FA biosynthesis, pneumolysin, and hemolysin that cause *Streptococcus pneumoniae* [12]. After reviewing the microarray of ΔluxS strains, gene clusters were observed where each cluster amplified in transcription overtime. The gene clusters were organized into chromosomal order that showed dysregulated genes arranged into separate groups assembled by distinct functions such as FA and phospholipid biosynthesis, energy metabolism, and virulence. The expression of gene luxS seems to affect FA production of phospholipids when the ΔluxS mutant strain was cultured overtime, the gene *accD, a FAS gene,* was upregulated in gene cluster SP0426.

The translation of genes luxS and accA can each affect bacterial FAS. Since Jia et al. found *luxS* deletion in *L. plantarum* KLDS1.0391 reduced the synthesis of FAs [13] and *accA* also affects FA output, this study attempts to demonstrate an interaction between *accA* and *luxS*. To describe a possible synergy between *accA* and *luxS*, E. coli (+)asRNA-*accA* transformants were exposed to glucose molecules, *and* then the qPCR products of *luxS were* quantified (luxS-qPCR). Two main hypotheses were tested in this study, including: 1) silencing *accA* and lessening glucose availability decreases *luxS* expression that downregulates the LuxS/AI-2 QS system and reduces biofilm formation, and 2) inhibiting *accA* intensifies antibiotic susceptibility of gram-negative bacteria because *accA* suppression degrades the OM and IM by disrupting FASII. The antibiotic susceptibility of *E. coli* (+)asRNA-*accA* expressing cell cultures was tested by implanting tetracycline, carbenicillin, and chloramphenicol-containing disks were in the cell cultures. The purpose of this study includes displaying a connection between bacterial metabolism (glucose-accA-FASII) and virulence (i.e. accA-luxS activity) to present an advantageous novel approach of using *accA* and *luxS* gene inhibitors as potential antimicrobial gene therapies for Gram-negative bacteria.

Figure 1 Plasmid Assembly and Gene Silencing of *accA*

Plasmid Assembly and Gene Silencing of the PCR products and the PTasRNA expression vector of the plasmid pHN1257 were digested with the restriction enzymes XhoI (upstream) and NcoI (downstream). After the restriction digestion, the antisense PCR product was ligated into the IPTG-PTasRNA inducible vector of pHN1257 at the multiple cloning site.

doi: 10.3390/ijms15022773, this article is an open-access article distributed under the terms and
conditions of the Creative Commons Attribution license (http://creativecommons.org/licenses/by/3.0/).
https://www.ncbi.nlm.nih.gov/pmc/articles/PMC3958881/figure/f6-ijms-15-02773/

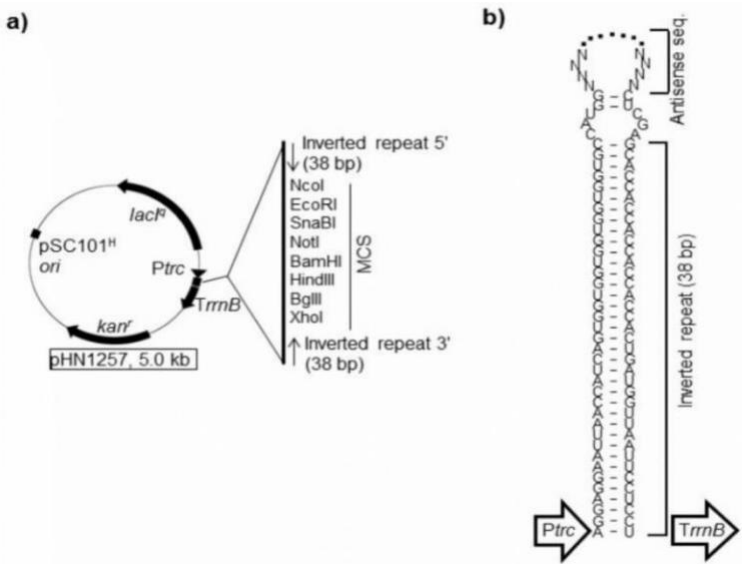

MATERIALS AND METHODS

BACTERIAL CELL CULTURE AND RNA EXTRACTION

The *Escherichia coli* TOP10 strain of cells was cultured and plated on 25 mL agar plates. The bacterial cells were inoculated into Luria-Bertani broth, enhanced with glucose concentrations of 200µM, 50µM, and 0µM. The cultures of 200, 50, and 0 micromolar (n=7) of glucose were measured for dsDNA and RNA OD260 concentrations and replicated seven times. Varying levels of glucose, including 15mM, 7.5mM, 5mM, and a control of glucose, were added to LB liquid with *Escherichia coli* cells. The plasmid pHN1257 was utilized to assemble the antisense expression vectors.

The recombinant plasmid pHN1257 for the expression of antisense RNA was plated with the kanamycin antibiotic and incubated at 37°C for 24 h. Cells grown on agar plates were inoculated into 4 mL of LB liquid media with (+) and (-) PTasRNA bacterial cells expressing asRNA for *accA* cultured with kanamycin. A total of 20 RNA extractions were completed with the Omega E.Z.N.A bacterial extraction kit.

cDNA PREPARATION

The author used the OneScript Reverse Transcriptase cDNA Synthesis kit by Applied Biological Materials Inc. or ABM. Approximately, 1µg of RNA from each sample, high glucose, medium glucose, low glucose, and (-) glucose were added to 0.5µM oligonucleotides(dT) (10µM). For asRNA and (-) RNA, 1 **µg** of each total RNA extract was added to the initial primer/RNA and reaction mixture. cDNA was also prepared for *luxS* quantification. The original primer/RNA mix consisted of 1µg of total RNA, 1µL of oligo(dt), 1µL of dNTP (10mM) mix, and nuclease-free water for a 20µL reaction solution.

PCR

A Promega PCR MasterMix kit at a volume of 25µL was added to the upstream and downstream primers, each of 0.5µL specific for the *accA* gene target. PCR amplification was repeated in triplicate. The concentrations of the two cDNA samples added to the PCR master mix were 190ng and 230ng plus nuclease-free water. A 2X and 1X upstream primer, 10µM 0.5– 5.0µl0.1–1.0µM, and a downstream primer, 10µM 0.5 to 5.0µl 0.1 to 1.0µM, DNA template 1–5µl less than 250ng, and nuclease-free water were mixed into a 50µl PCR reaction mixture. The PCR thermocycler completed 40 cycles of amplification instead of 35 cycles.

AGAROSE GEL ELECTROPHORESIS AND PLASMID ASSEMBLY

The conditions of the PCR products, without primer dimers and contamination for the target gene *accA,* were detected through agarose gel electrophoresis. The PCR products were confirmed without primer dimers, and contamination, the PCR products, and the PTasRNA expression vector of the plasmid pHN1257 were digested with the restriction enzymes XhoI (upstream) and NcoI (downstream) (New England Biolabs XhoI- catalog R0146S- 1,000 units and NcoI- catalog R0193S- 1,000 units) (Fig. 1). Each microcentrifuge tube was placed in an incubator for 30 min at 37°C. A heat block was heated to 90°C. The PCR products of the *accA* gene were ligated into the pHN1257 plasmid by mixing 1µL of the DNA insert with 2µL of the plasmids, adding 5µL of the ligation mix, and then placing the tubes into a heat block at 90°C for 15 min (Takara Ligation Kit 6023).

REAL-TIME PCR

The author enhanced each bacterial sample with glucose concentrations of 15mM, 7.5mM, 5mM, and 0mM (n=3). The cDNA from H-glucose, M-Glucose, L-glucose, and the control (-) glucose was diluted in a 1:8 serial dilution. A 10-fold dilution of standards was prepared for bacterial samples transformed with (+) asRNA-inducible plasmids and exposed to high to low volume of glucose. The amount of gene expression for *accA* and the target gene *luxS* was measured using absolute quantification methods of qPCR. The diluted cDNA was pipetted into a transparent 96 well plate. A 0.4µL of each primer pair mixture was pipetted into a microcentrifuge tube with 10µL of SensiMix SYBR MasterMix, and with 1.2µL of DEPC water. The SYBR reaction mixture of 12µL was then pipetted into the wells with diluted and undiluted cDNA. The optical film was sealed to the plate. The PCR plates were centrifuged for 2 min at 2500 rpm to reposition all liquids to the bottom of the wells. The real-time PCR amplification protocol from the Roche Lightcycler 480 was used.

THE qPCR ABSOLUTE QUANTIFICATION OF LUX-S

Bacterial cells were transformed with the pHN1257 plasmid expressing asRNA to inhibit the genetic expression of *accA*. Triplicates of qPCR were performed to quantify the gene copies of *luxS*. The author added 25µM and 5µM concentrations of glucose to the bacterial samples expressing antisense RNA for the inhibition of the gene *accA.* RNA was extracted from cells grown with 25µM glucose and 5µM glucose. The cells grown with glucose in the medium were also transformed with antisense expressing IPTG-PT-asRNA inducible pHN1257plasmids. Cells were cultured without (-) glucose, but the expression of *accA* was also inhibited by (+) asRNA. A control without (-) glucose and (-) asRNA was compared for each sample. The number of gene copies for *luxS* was measured using the qPCR amplification protocol and absolute quantification (Roche Lightcycler 480).

ANTIBIOTIC RESISTANCE TEST

Competent T7 bacteria cells were transformed with the inducible vector termed pHN1257, expressing antisense RNA to inhibit the gene *accA.* The newly remodeled bacterial cells were plated in nutrient agar medium consisting of the antibiotic kanamycin. Three to five colonies from the pHN-1257-asRNA-*accA* bacterial transformants were selected and cultured in LB broth, enhanced with kanamycin for 18 to 24 h at 37**°C** in a shaking incubator. A control group that did not express asRNA for *accA* was cultured in LB broth overnight at 37**°C**. One hundred microliters of the pHN1257- asRNA-*accA* and from the control group were pipetted into nutrient agar Petri dishes (N=64) containing 50 micromolar of kanamycin (50µg/mL) antibiotic for the sample of pHN1257-asRNA-*accA*. A swab was used to spread 100**µL** of each

experimental (with asRNA) and the control (without asRNA) onto the agar plates to form a lawn of bacterial growth. The six millimeter-sized disks contained five microliters for each of the three consecutive antibiotics, including tetracycline (10µg/mL), carbenicillin (100µg/mL), and chloramphenicol (25µg/mL). Each group of eight disks was prepared with tetracycline carbenicillin, and chloramphenicol. The antibiotic disks were placed on the agar plates. The bacterial cultures grew for 18-24 h at 37oC. The zones of inhibition for each of the discs (N=64) was measured in mm and compared to specific criteria for determining antibiotic resistance and susceptibility of bacteria.

STATISTICAL ANALYSIS

The figures were constructed with the Sigma Plot, in 14th edition, Microsoft excel, and the 8th edition of GraphPad Prism. The mean and standard deviations were calculated by Microsoft Excel and GraphPad Prism. The p values and the ANOVA results were produced through GraphPad Prism. The standard curves for the absolute quantification of the genes accA and luxS were generated through Microsoft excel with linear regression coefficients added and calculated for each standard curve for the absolute quantification of accA and luxS. The antibiotic resistance test was analyzed, given descriptive statistics, and generated paired-t-test results through the OriginPro 2019B software. A t-test and a density graph for antibiotic susceptibility of pHN1257(+) asRNA for accA was produced through OriginPro 2019B.

RESULTS AND DISCUSSION

THE EFFECT OF GLUCOSE ON THE RNA CONCENTRATION AND THE EXPRESSION OF *accA*

To confirm the effect of extracellular glucose on intracellular RNA transcription and *accA* expression, glucose was added to *E. coli* liquid cultures. As the glucose concentration increased, the transcription of *accA* was amplified. After culturing *Escherichia coli* with varied concentrations of glucose, the RNA concentrations for each sample measured were 1392, 797, 608, and 199 ng/µL for H-Glucose (15mM) , M- Glucose (7.5mM), L-Glucose (5mM), and the control, respectively, (Fig 3). The RNA of each bacterial sample enhanced with glucose was extracted, and the concentrations determined (N=20, 335.4 ± 329.2). The level of *accA* by qPCR analysis, in units ng/µL, included: 4210, 375, 1500, and 196 for H-glucose, M-glucose, L-glucose, and the control, respectively (Fig 3).

After loading a 96-well plate with 8-fold dilution standards for each sample, the standards of each sample were used to calculate a standard curve. The standard curves were used to perform absolute qPCR quantification of *accA* gene copies. The number of qPCR *accA* products ranged from 11-186, 5-18, and 0-79 gene copies for high-glucose, medium-glucose, and low-glucose/control, respectively, (N=12, 48±38). When comparing 200 µM-glucose bacterial samples to the control groups, the difference between the samples was statistically significant

(p=0.038) (Figs 3-4). The cells grown at 200µM of glucose yielded a more substantial and excessive yield of dsDNA than cells cultured without glucose (Figs 3-4). The residual plots of [RNA] versus [*accA*] were nonlinear with a nonconstant variance that showed increased distance between the error and predicted values (Fig 5).

After adding glucose, RNA transcription augmented because increased carbon uptake induces intensified *accBC* and *accD*1 transcription and by controlling the flux of the tricarboxylic acid (TCA) cycle the production of malonyl-CoA increases [14]. More available carbon nutrients from glucose addition increased the transcription of *accA,* as reflected in the qPCR results. Adding glucose to the liquid cultures amplified the activity of the CT to transfer more carboxyls to acetyl-CoA for conversion into malonyl-CoA. The glucose escalated *accA* expression. Acetyl-CoA carboxylase (ACC) is a biotin-dependent carboxylase. The ACCase complex consists of a biotin carboxylase (BC), carboxyltransferase (CT), and a biotin-carboxyl carrier protein (BCCP) subunit. The BC of *E. coli* is bonded into a dimer (Fig 2).

Figure 2 BC of *E. coli* is bonded together in a dimer (*Retrieved from Reference 15)***.** Each dimer has an active site oriented at 25Å from the region of interaction. This dimer interface is composed of distant communications between each of the two active sites in a dimer. The two monomers of the BC dimer may share the responsibility of inducing catalysis. One of the BC monomers can bind the substrate during its initiation of the reaction, while the second monomer disperses the product.

Figure 3 Glucose concentration versus RNA Glucose concentrations of 15mM, 7.5mM, and 5mM with the control samples each yielded RNA concentrations in ng/µL, 1392, 797, 608, and 179, respectively. A) The bacterial sample with 15mM glucose yielded the highest substantial measure of RNA, noting a proportional relationship between glucose and genetic expression of *E. coli*. B) The results display the qPCR results for 15mM, 7.5mM, 5mM, and control. The samples with 15mM and 5mM glucose showed the highest genetic activity of *accA* transcription, measuring *accA* concentrations of 4,210 ng/µL and 1,500 ng/µL, respectively. The *accA* qPCR concentrations for 7.5mM *accA* equaled 372 ng/µL and 196 ng/µL quantities for the control. C) The analysis displays the OD260 measure of DNA results for samples of *E. coli* grown in medium enhanced with 200µM, 50µM, and 0µM of glucose.

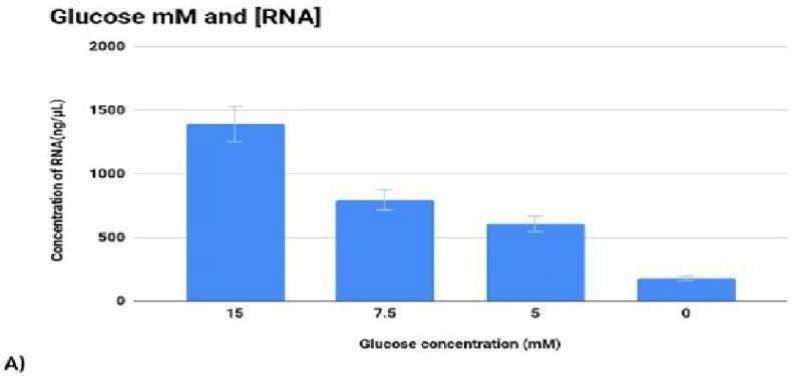

A)

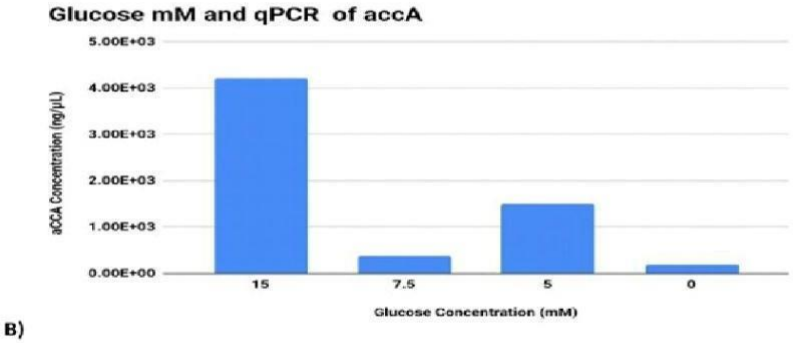

B)

C)

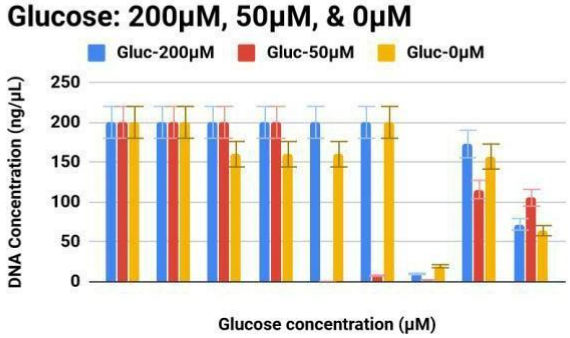

Figure 4, RNA Concentrations vs. Glucose Concentration A) The enhanced *E. coli* bacteria cultures (n=3) with 200µM, 50µM, and a control of glucose (59±49). B) at 50µM of glucose in a bacterial sample, the highest yield was 566ng/µL, 200µM, 117ng/µL of RNA was produced, and the control measured 76ng/µL of RNA.

A)

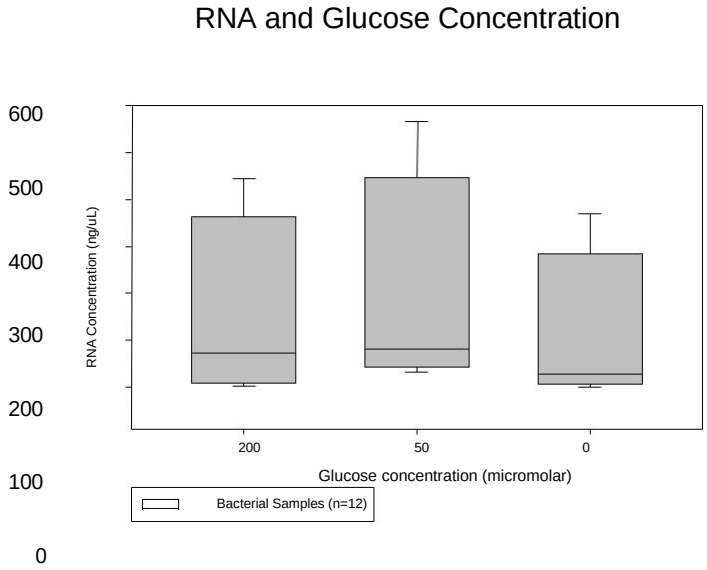

B)

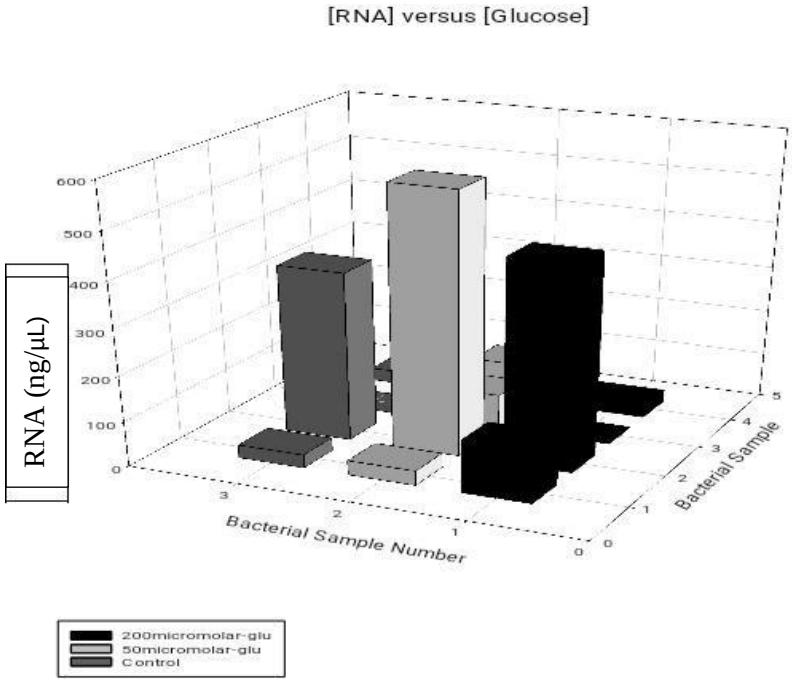

Figure 5 Predicted and Actual Residuals A) The QQ plot of RNA concentration versus *accA* exhibits means that are normally distributed. B) The homoscedasticity of [RNA] and [*accA*] is nonlinear due to the size of error that varies across values of [RNA] and *[accA*]. C) The residual plot resembles heteroscedasticity where residuals increase as the predicted values move from 0 to 800 ng/µL for [RNA] and [*accA*].

A) B) C)

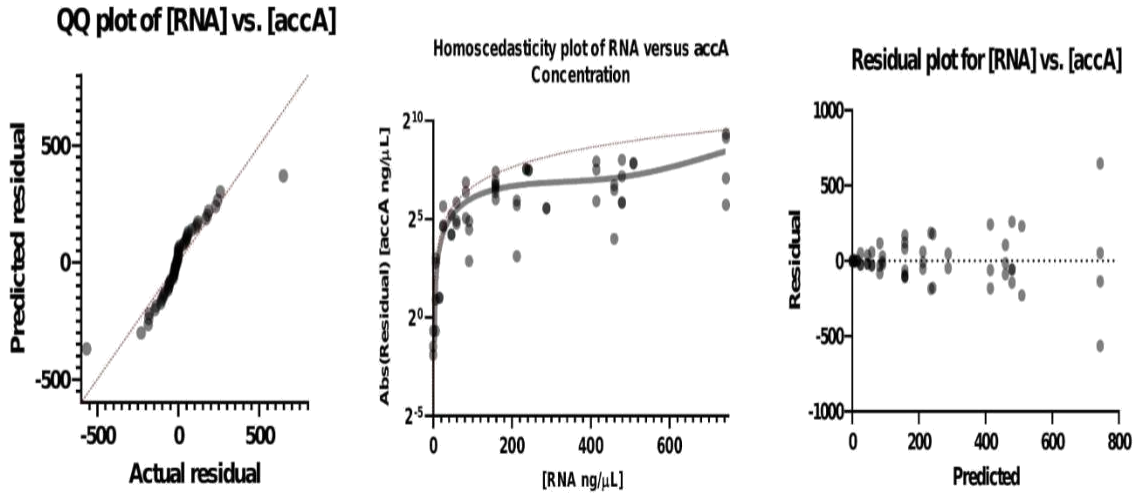

The biotin-dependent ACCase enzyme performs a crucial function for catalyzing fatty acid metabolic activity. The ACC complex completes two enzymatic reactions in two half-reaction steps. The first step is catalyzed by a biotin carboxylase (BC) that carboxylates an N1' atom of a biotin vitamin cofactor, utilizing ATP and carbon dioxide bicarbonate [16]. Biotin or vitamin H covalently bonds to a lysine side chain residue located in the BCCP subunit. The second step uses a carboxyl transferase (CT) to transfer carbon dioxide from a carboxybiotin to a carboxyl group. The increased glucose supplementation provided excess carboxyl groups and ATP needed for the BCCP of an *E. coli* ACC to use its thumb appendage (Fig 6). As biotin binds to the BCCP, the thumb attaches to biotin. The thumb fortifies the BCCP, tightening the bond between biotin and the BCCP. By increasing glucose, more energy from ATP was available for the ACCase enzyme to link the BCCP thumb to biotin.

Eliminating one of the dimers of BC renders it inactive. Each BC dimer has an active site oriented at 25Å from the region of interaction of the dimer [17]. This dimer interface is composed of distant communications between each of the two active sites. The two monomers of the BC dimer may share the responsibility of inducing catalysis. One of the BC monomers can bind to the substrate during the initiation of the reaction, while the second monomer disperses the product. However, the BC dimer during the first half reaction does not exhibit cooperative behavior confirmed by enzyme kinetic analysis.

Biotin carboxylase has 449 amino acid side chain residues. The 449 residues of BC are split into three domains. The three domains include a domain at the N- terminus, an ATP-grasp or a B-domain, and a C-terminal domain. The Met1-lle103 residues represent the N-terminal domain that consists of a β-sheet, five parallel strands, and four α-helices. The ATP grasp contains the residues Val131-Tyr203, 3 β-sheets, and two α-helices [7]. BC has residues Arg208-Lys449 in its C-terminal domain. The BC subunit is composed of 8 antiparallel β-sheets, 3 antiparallel β-sheets, and 7 α-helices [7]. Each monomeric section of the BC dimer has an active site where the residues are not shared between the monomers.

Glucose also provided the carboxyl groups required for the BCCP to transfer a carboxyl to CT. The BCCP of bacteria closely resembles the ACC2 of human ACC, but human ACC2 does not contain a thumb extension [16]. Human BCCP is less restricted and can interact more with the BCCP of *E. coli*. In humans, the presence of a thumb inhibits biotin from binding to the human holocarboxylase synthetase or HCS [16]. However, in *E. coli,* the thumb does not interfere with biotin, forming a bond with an enzyme called *E. coli* BirA. Biotin is needed for all biotin-dependent carboxylase reactions.

Figure 6, The BCCP of *E. coli* ACC uses a thumb appendage (*retrieved from reference 18***). A)** The "thumb" of a BCCP. **B)** As biotin binds to the BCCP, the thumb attaches to biotin. **C)** The BCCP transfers the carboxyl to the CT. The thumb fortifies the BCCP, tightening the bond between biotin and the BCCP.

(BCCP)

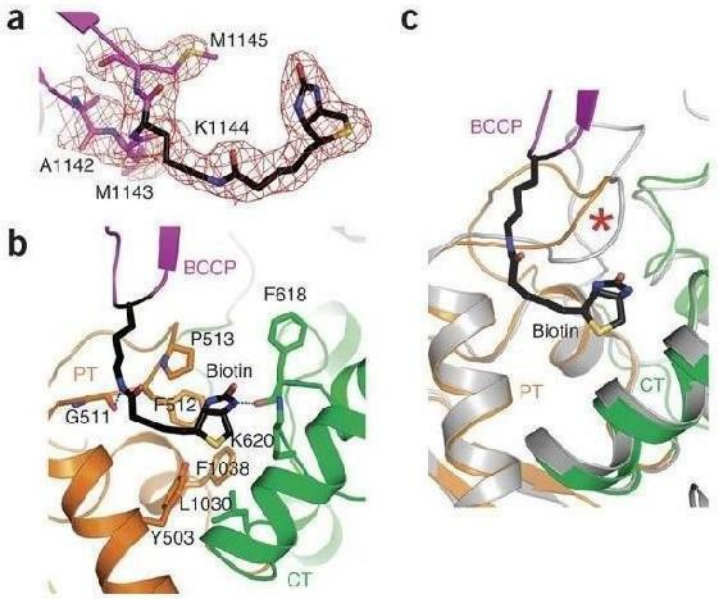

If a carboxyl is not present, then biotin cannot attach to the CT subunit [17]. This prevents the loss of ATP as a source of energy for BC-to-CT coupling reactions. The *E. coli* samples that were enhanced with glucose produced the highest concentration of *accA* and RNA because the glucose produced more ATP for the BC-to-CT interaction to occur. The glucose contained increased pyruvate molecules that yielded more carboxyl groups and ATP for the BC-CT interaction. The increased access of carboxyl groups induced the amplified attachment of biotin to the CT. The CT subunit has an N and a C domain. Each of the two subunits has a crotonase fold, which is a β-β-α superhelix [16]. At the interface of the CT dimer, there is an active site present.

The CT subunits are α2β2 heterotetramers [16]. The CT subunits are required to bond as a dimer to activate CT and catalyze the second half reaction (Fig 7). The X-ray crystal structure of the CT shows a bond between the intermediate and the product of the response [17]. Every biotin-dependent enzyme requires two half-reactions that have structurally isolated and separated active sites [17]. It has been confirmed that separated active sites are physically produced in this orientation to regulate the interaction with biotin, which stabilizes the interaction of biotin with the BC to CT reactions. BC, BCCP, and CT mimic a ping-pong-ball-type interaction over a distant gap of separation between the carboxylase and transferase reactions [19].

Figure 7 The CT domain, has an N and a C domain (*this figure was retrieved from the Protein Data Bank of Europe and originally published in reference 20*)**.** Each of the two subunits has a crotonase-fold. This is a β-β-α superhelix (Tong, 2013.) At the interface of the CT dimer of its domain, there is an active site present. The CT subunits are α2β2 heterotetramers. The CT domains are required to bond as a dimer for the CT to be active and catalyze the second half reaction. (color-grey=β/AccD, color-blue=α/AccA.)

(CT)

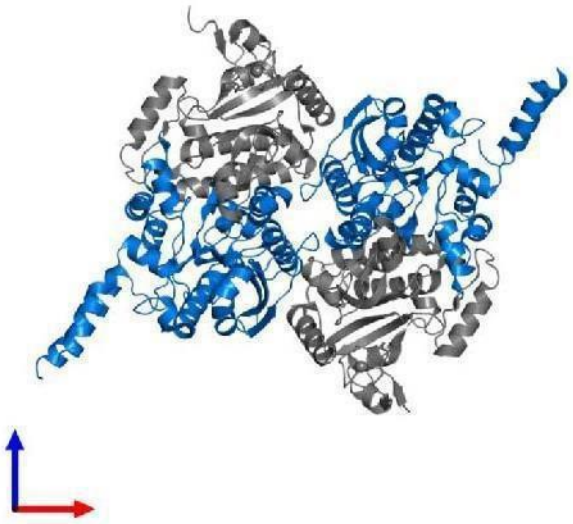

There was a reduction in *accA* and RNA activity because of the reduced availability of carboxyl groups after decreasing glucose. When carboxyl groups are supplied by glucose, the ATP grasp of BC can appear as a closed conformation. When there are less carboxyl substrates bound to the biotin carboxylase, the ATP-grasp domain appears as an open conformation that extends from the primary protein structure. When the glucose was decreased, fewer carboxyl substrates could bind, and the ATP-grasp domain remained in an opened configuration. Reducing the volume of glucose provided less ATP availability.

Less ATP lowers the activity of ATP with the ATP-grasp monomer. When ATP binds to the ATP grasp domain, it rotates at a 45° angle to capture the ATP and grasp it into its active site [21]. When the BCCP domain of human ACC2 was placed over the C-terminal alpha atoms of the image of the *E. coli* structure, the crystal violet image discovered the human ACC2 did not have a “thumb.” The “thumb” is a loop with eight amino acids that extend from the BCCP-C-terminus domain [21]. The BCCP and BC of *E. coli* become bound together at an angle of resolution equal to 2.49 Å [7]. The BCCP and BC are new sites that can be targeted with antibiotics to reduce the activity of acetyl-CoA carboxylase. When ablating *accA* gene expression, the alpha-subunit (AccA) of the CT for the ACCase enzyme can become absent and disrupt the BC-to-CT interaction required for catalyzing fatty acid synthesis. Fatty acid synthesis is catalyzed by the CT conversion of acetyl-CoA into malonyl-CoA.

Generally, BC, BCCP, or CT are all bonded together as a multi-subunit protein or as separate subunits. However, the orientations of the ACCase subunits relies on the type of organism and the class of the ACCase enzyme. BC and BCCP are conserved conformational structures. The conformation of the CT subunit, instead, depends on the behavior of the chemical substrates. The ACCase enzyme is biotin-dependent for catalyzing fatty acid synthesis. Biotin consists of a C, N, and a S cyclic ring linked to a five-carbon fatty acid chain. Biotin is a cofactor that is required for metabolism. Biotin is called vitamin H, which is bound to a lysine side chain residue of a biotin-dependent enzyme [22]. The biotin to protein bond assists with carboxylation and decarboxylation activities. To catalyze the biotin-dependent carboxylase reactions, BC and CT must interact with the biotin cofactor. Bacterial ACCase enzymes encase four subunits: BC at 50kD, BCCP subunit with 17kD, and two subunits called alpha and beta, weighing at 33 kD for each component required for the CT reactions [16]. The ACCase enzyme has a stoichiometric ratio of 2:4:2 for BC, BCCP, and CTα with CTβ, respectively.

qPCR RESULTS OF THE ANTISENSE RNA INHIBITION OF TARGET GENE *accA*

For confirming the inhibition of *accA*, *E. coli* cells were transformed with pHN1257 plasmids carrying the insert for asRNA transcription of *accA*. The production of antisense RNA required the ligation of the PCR product for the antisense gene insert, *accA,* into the plasmid pHN1257 (Fig. 1). The reengineered pHN1257 amplified the expression of asRNA of *accA*. The total RNA concentration for the control (-)asRNA-*accA* equaled 739.44 ng/µL. The control (-)asRNA-*accA* yielded a miRNA concentration of 334.98 ng/µL. The RNA concentration for transformed bacterial cells with the asRNA of the *accA* pHN1257plasmid was 279.28ng/µL. The miRNA concentration of the cells with asRNA-*accA* measured 240.90 ng/µL. The gene of *accA* was successfully suppressed by asRNA in vitro with 63 ng/µL of qPCR measured for bacterial cells (n=3, 37.8 ± 35.6). The real-time PCR (qPCR) results for bacterial cells without the asRNA for *accA* ((-)asRNA-accA) yielded 421.69 ng/µL for *accA.* There was a 147 % (95% CI, [63, 421.69]) difference between cells without asRNA expression versus cells with asRNA-accA inhibition (p=0.027).

FAS requires catalysis by acetyl-CoA carboxylase transferase, which transfers carboxyl to acetyl-CoA to produce malonyl-CoA [23]. The FAs are produced after CT, encoded in *accA and accD*, transfers a carboxyl group to acetyl-CoA, forming malonyl-CoA (Fig 8). This catalyzation requires energy from ATP, access to bicarbonate, and the vitamin H cofactor of biotin. ATP from glucose is the most significant source of energy that is needed for most metabolic activities. The inner membranes (IM) for gram-negative bacteria are composed of phospholipid bilayers. The phospholipid (PL) bilayer is constructed by FASII [2]. The first phase of FASII includes the carboxylation of acetyl-CoA, which forms malonyl-CoA through a biotin carrier protein (BCCP) and the acetyl-CoA carboxylase transferase (CT) enzyme. FASII includes separate subunits that interact. FASI proteins are expressed as cohesive and connected domains on a multi-polypeptide chain. *E. coli* has an acetyl-CoA carboxylase, which is a part of the FASII category.

The CT catalyzes the transfer of a carboxyl group to acetyl-CoA, producing malonyl-CoA after BCCP transports the carboxyl to CT. The BCCP carrier has two main domains. It has an N-terminal and a C-terminal domain. The C-terminal domain consists of a biotin cofactor that is substrate-like. The role of the N-terminus of the biotin carrier is presently not completely elucidated. However, the N-terminal domain can attach and bind to biotin. The utilization and function of the N-terminus seems to link and fortify the carboxyl to biotin bond. The transfer of the carboxyl from the biotin protein carrier (BCCP) through the carboxyltransferase (CT) to acetyl-CoA is completed by two reactions [24]. The first half reaction that uses the biotin carboxylase (BC) initiates the addition of a carboxyl to biotin through its covalent bond to BCCP.

The second reaction is catalyzed by CT, which repositions a carboxyl to acetyl-CoA and yields malonyl-CoA. By inhibiting the *accA* gene with a reengineered IPTG-PT-asRNA vector, the absent AccA subunit of CT could not interact with BCCP. Less interaction between BCCP and CT can lower the production of acyl-ACP from malonyl-ACP because less CT conversions of acetyl-CoA into malonyl-CoA would occur that are required to catalyze FAS for elongation of acyl-ACP. The complexes of acetyl-CoA carboxylase enzymes catalyze the carboxylase and transferase reactions. The carboxylase enzymes catalyze the addition of a carboxyl to a biotin prosthetic group of the biotin carboxylase carrier protein (BCCP) [6]. The carboxylase transferase (CT) also initiates and transports a carboxyl from the BCCP to an acyl group, which forms acyl thioesters.

Figure 8, Formation of Malonyl-CoA ***(****This figure was retrieved from reference 25 and originally published in the Journal of Biological Chemistry),* The acetyl-CoA carboxyl transferase, the AccA and AccD, and the alpha and beta subunits of the AccABCD complex transfers a carboxyl group from pyruvate to acetyl-CoA to form malonyl-CoA. Malonyl-CoA enters the fatty acid synthesis pathway, elongating fatty acids into long-chain fatty acids into phospholipids. The covalently bound biotin of BCCP carries the carboxylate moiety. A biotin carboxylase (BC) carboxylate an N1' atom of a biotin vitamin cofactor, utilizing ATP and carbon dioxide from bicarbonate. Biotin or vitamin H has a covalent bond to a lysine side chain residue located in the biotin carboxyl carrier protein or the BCCP subunit. The second step uses a carboxyltransferase (CT) to transfer carbon dioxide from a carboxybiotin to a carboxyl group. The CT moves the carboxyl group to acetyl-CoA, producing malonyl-CoA.

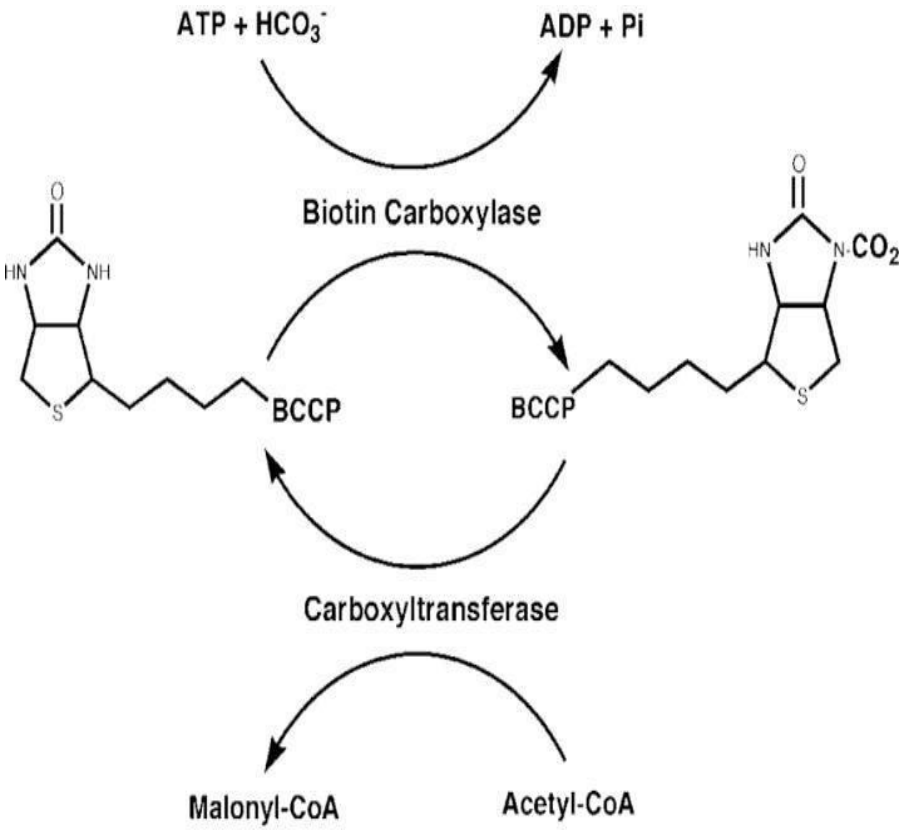

Inhibiting *accA* lowered the expansion of fatty acid production because lessening ACCase activity shortens the length of the acyl chain, which can increase or decrease in elongation. Bacterial cells, in response to low temperatures or toxicity, can change the ratios of their acyl chains through saturation to unsaturation, from cis to trans-double-bonded carbons, and from branched to unbranched stacks of acyl chains [26]. Lipids are the central building blocks of the inner cytoplasmic membrane. Lipids maintain the structure of bacterial cells, increase survival, and increase growth, and allow the passage of hydrophobic units via increased membrane permeability. The lipid acyl chains that are produced during FASII construct a more fluid and permeable bacteria cells (Fig 9).

Environmental fatty acids can also affect the fatty acids of the bacterial plasma membrane. *S. aureus* can absorb fatty acids from its environment and increase its rate of survival and growth even after antibiotic treatment of a fatty acid synthetic pathway. The biofilm of bacterial cells consists of larger concentrations of fatty acids that increase fluidity, isolating the bacterial community from a tumultuous environmental condition [26]. Fatty acid synthesis requires large quantities of energy and further access to phospholipids provided by the added glucose, which increases the activity of the ACCase enzyme. The asRNA inhibition of *accA* can reduce the output of fatty acids that can negatively affect the biofilm yield and its composition. Fatty acids stabilize the plasma membrane lipid bilayer for developing the early stages of biofilm.

Biofilm plays an intricate role in the origin and source of infection. Biofilm allows the movement of pathogenic bacteria to become more rapid and spread an infection into the blood circulation [61]. Researchers treated mutant cultures with kanamycin and found that the biofilm showed a reduction in antibiotic resistance. However, after 250 generations, the resistant mutant bacteria increased growth at the surface and the base of the biofilm [27]. Bacterial colonies within a biofilm are resistant to antibiotics. Because the extracellular biofilm matrix prevents the penetration of antibiotics, is mostly anaerobic, or lacking oxygen, bacteria within the biofilm are more tolerant of antibiotics [28].

Bacterial cells in the biofilm have greater access to nutrients and oxygen than in a culture medium. Higher levels of fatty acids are present during the early growth phase. In addition, the large concentrations of DNA present in the biofilm serve to maintain a more cohesive matrix and a higher quality of the biofilm [29]. Bacterial cells located in the biofilm versus planktonic bacterial cells possess higher concentrations of fatty acids. The higher access of fatty acids increases tolerance to various temperatures, more stacking of bacterial cells, and more stable lipid bilayers. A heightened presence of long-chain fatty acids leads to the increased orientation of fatty acids in the lipid bilayer, amplifies the links between acyl chains, and stabilizes the lipid bilayer [26]. The fatty acids produced will form a more fluid membrane, and this fluidity causes the biofilm to expand. As the biofilm broadens, increased LuxS activity is

needed to synthesize, and release AI-2 signals for quorum sensing.

Figure 9 for Long-Chain Fatty Acid Synthesis, An acyl-group, or ACP, is added to the malonyl-CoA and converted into ketoacyl-ACP by an added carbon dioxide. The Beta- ketoacyl-ACP is reduced and gains hydrogen into Beta-hydroxyacyl-ACP. The Beta- hydroxyacyl-ACP is dehydrated, losing a molecule of water, to alter into Enoyl-ACP, which forms Acyl-ACP by losing two hydrogen protons. Two carbons for FA elongation are added per cycle of FAS.

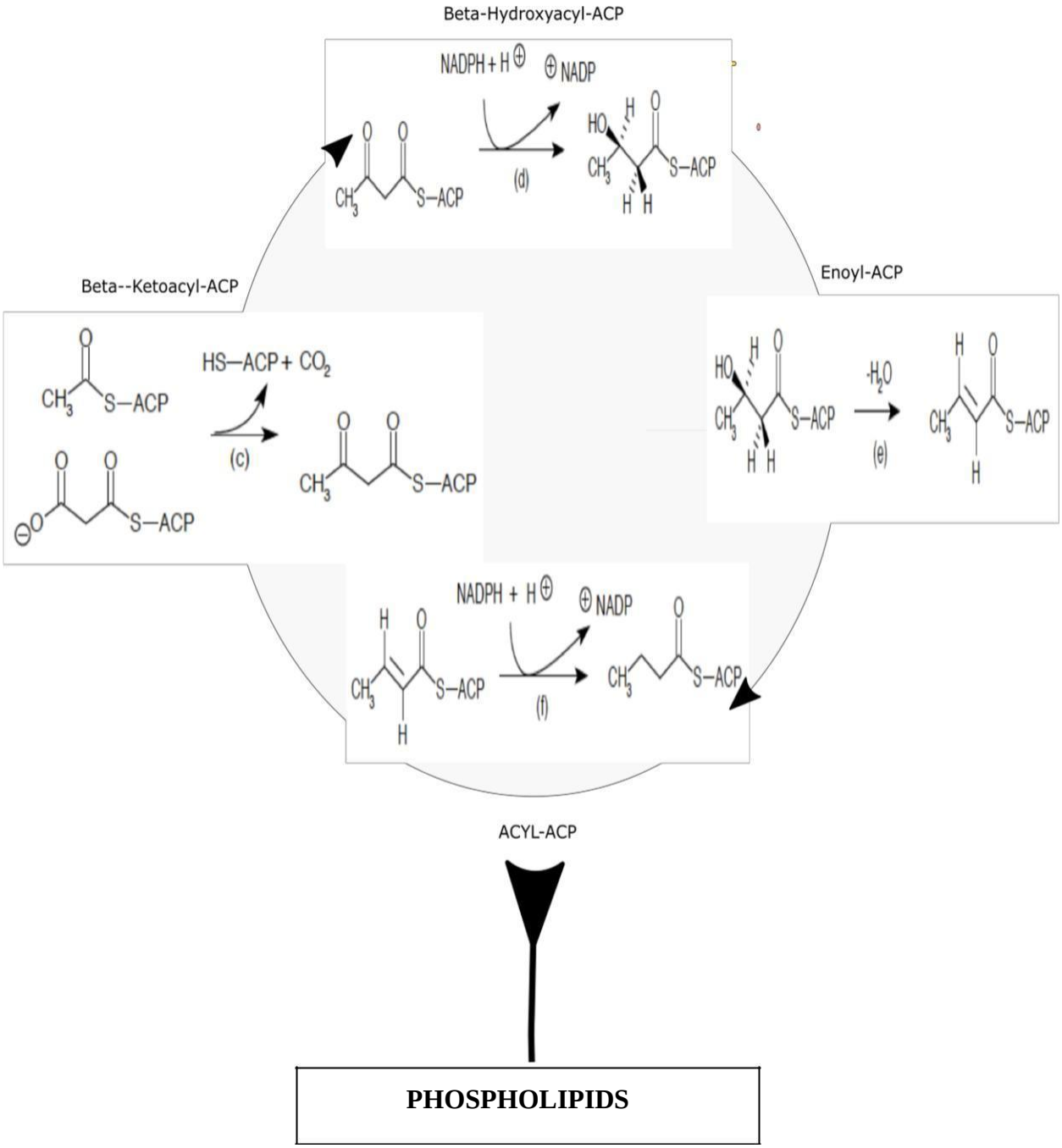

qPCR ANALYSIS OF *luxS* GENE EXPRESSION

LuxS synthesizes AI-2 QS signals needed to form biofilm, regulate gene expression, and release virulent factors. To determine the effect of *accA* inhibition on *luxS,* a qPCR analysis measured the number of l*uxS* gene copies after inhibiting *accA* while altering glucose availability. *E. coli* cells were transformed with antisense pHN1257 expressing IPTG-PT-asRNA-accA plasmids and cultured with 5µM-25µM of glucose. Glucose increased the rate of transcription and *accA* inhibition decreased the overall production of nucleic acids (Fig 10). Cell samples with 5µM glucose-(+)asRNA produced a high level of the *luxS* gene. The gene copy values of *luxS* for (+) glucose-asRNA and (+)-asRNA were quantified. For the results, (-) glucose-(+)asRNA samples produced a gene copy number of 199 (n=3, 277 ± 37) and $1x10^6$ *luxS* gene copies for the control ((-) glucose-(-)asRNA).

The asRNA of *accA* did lower the levels of *luxS* without glucose additives. For the 25µM glucose-(+)-*accA* asRNA and 5µM glucose (+)-asRNA-*accA* produced 39,810 and 316,228 gene copies of *luxS*, respectively. In the control samples, (-) glucose-(-) asRNA (n=3, 658,114 ± 483,499) and 5µM glucose- (+)asRNA (n=3, 171571±204574) exhibited the highest level of *luxS* expression ($p<0.05$, $p=0.025$). The 5µM glucose-(+)asRNA-accA produced 316,228 gene copies, and the control generated $1x10^6$ qPCR products. Wang et al. found that adding 0.8% glucose to the bacterial culture and growth medium increased the activity at the promoter site of the *luxS* gene [30]. Jesudhasan et al. proved that higher levels of autoinducer-2 did not necessarily lead to increased gene expression of *luxS* for *Salmonella typhimurium* when cultured in excess concentrations of glucose [31].

LuxS expression is an essential component for cell growth, quorum sense, and biofilm formation. The excess AI-2, produced by LuxS, sequesters, and induces many bacterial cells to exchange AI-2 signals [32]. AI-2 fills the extracellular space when the bacterial population increases in growth [33]. Bacterial cells detect the excess AI-2, assess cell density, and then signal the cessation of gene expression. Quorum-sense activity monitors and regulates gene expression through a positive feedback loop. This positive feedback is triggered by the peripheral and internal accumulation of AI-2. Quorum sense signal exchanged between bacterial cells monitor the genes responsible for organizing activities executed through different bacterial groups. Activities completed through quorum sense signaling include bioluminescence, spore formation, antibiotic excretion, creating biofilm, and releasing factors for virulence [33]. For example, the malfunctioning of *fsr* that resides in the quorum-sense gene locus for *E. faecalis* decreases biofilm formation [34].

Figure 10 Effect of glucose on the rate of transcription inhibition with asRNA and frequency of nucleic acid production A) from the control to 25 µM glucose exposure, bacteria cells transcribed DNA at an amplified rate. As the glucose concentration increased to 50 micromolar, the rate of transcription reached a sustained equilibrium with no new nucleic acid production or activity. B) asRNA caused gene inhibition of *accA.* The samples expressing asRNA inhibition of *accA* produced 16% (95% CI, [199, 1x10^6]) of the total yield of nucleic acids. Samples not represented asRNA inhibition yielded 83% (95% CI, [199, 1x10^6]) of the total amount of nucleic acids.

A.

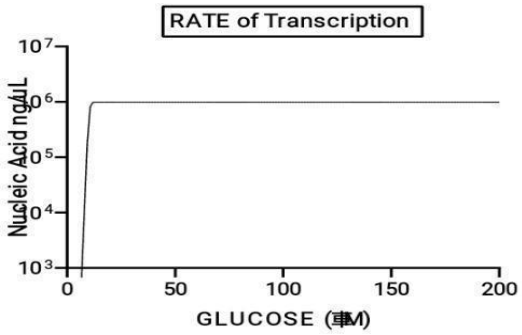

B.

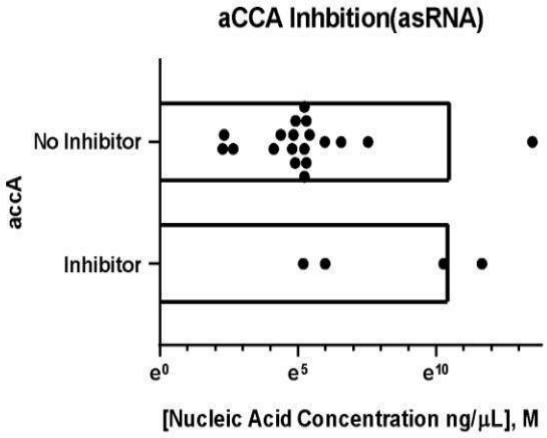

E. coli produces quorum-sense signals that regulate gene activity and growth. *E. coli* and many gram-negative bacteria regulate the influx and output of AI-2. In *E. coli*, the transporter and transmembrane complex called LsrABCD, an ATP-binding cassette importer, controls AI-2 uptake. LsrABCD contains transmembrane permease proteins, nucleotides for binding proteins, and a periplasmic solute to bind proteins. The repressor of LsrABCD and LsR is a kinase that is a part of the QS system of AI-2. Cyclic AMP/cyclicAMP receptor proteins regulate the *lsr* operon. The expression of cyclic AMP/cyclic AMP receptor proteins occurs by the positioning of *lsrK* and *lsrR* upstream of the *lsr* [35]. Lsrk that is a kinase located in the cytoplasm, phosphorylates AI-2, and then the Lsrk attaches to the *lsr* repressor.

In an intercellular process called quorum sense (QS) signaling, bacterial cells release AI-2 signaling molecules for detecting cell density and to regulate gene expression. Studies have shown AI-2 as a signaling molecule that regulates cellular processes in *Salmonella*. The activated AI-2 suppresses the *lsr* repressor, termed LsrR. After the activity of the *lsr* repressor is inhibited, the release of AI-2 proliferates via the autoinducer-activated expression of LuxS. AI-2 accumulates, monitors cell growth by permitting bacterial cells to sense the excess AI-2, and then terminates cell growth. Excess AI-2 distributes quorum sense signals between bacterial cells, which notifies cells of limited nutrients, surface area, or available space. AI-2 is dependent on the genetic expression and translation of *luxS* (Fig 11).

Figure 11 Regulatory mechanisms of the LsrR/phospho-AI-2 system in *E. coli* (Retrieved from reference 35). The AI-2 uptake repressor LsrR represses the *lsr* operon containing *lsrACDBFG* and the operon of *lsrRK*. AI-2 can reenter the cell through the expression of LsrACDB. When the LsrK kinase phosphorylates an imported AI-2, the phosphorylated AI-2 binds to LsrR and terminates its repression of *lsr* transporter genes, inducing their expression. These regulatory steps trigger increased AI-2 uptake. (DPD=4,5-dihydroxy-2,3-pentanedione) **

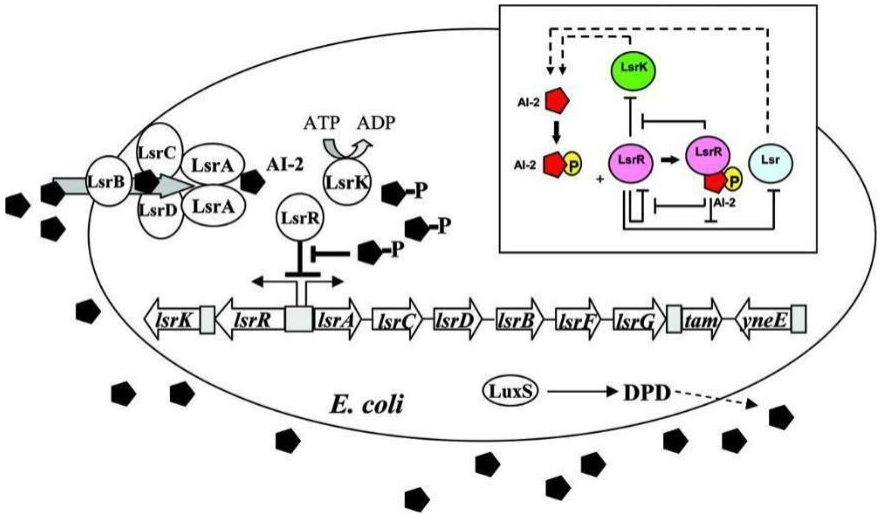

The inhibition of *accA* and decreasing the accessibility of glucose lowered the activity at the *luxS* promoter site. LuxS is an AI-2-synthesizer. The escalating output of AI-2 amplifies *luxS* transcription. Widmer et al. (2012) found that the *luxS* mutant strain, PJ002, exhibited increased bacterial cell growth after adding 25μM of AI-2, which was not present in the phosphate-*buffered* saline or PBS buffer control solution [36]. The heightened genetic activity of *luxS* after glucose supplementation with or without the inhibition of *accA* can confirm the metabolic dependency of the LuxS/AI-2 QS system. Inhibiting *accA* and decreasing glucose lowered the expression of *luxS,* where less activity of the LuxS/AI- 2 QS system can reduce biofilm consistency and degrade cell structure.

The reduced function of CT via *accA* extirpation can lessen the output of fatty acids that limit a bacterium's expression of virulence, initial adhesion to a surface, and its mobility [37]. When ablating *accA*, less *luxS* was produced where reduced fatty acid synthesis can decrease LuxS (Fig 12). The declining activity of LuxS can lower the release of AI-2. Less AI-2 blocks quorum sense activity that detects cell density needed to activate or inhibit gene expression. Many bacteria form fatty acyl-homoserine lactones, or acyl-HSLs that operate as quorum-sensing signal molecules, bind to signal receptors, and monitor gene expression. The fatty acyl groups are developed from fatty acid biosynthesis and elongation [38]. By inhibiting *accA* with asRNA interference, the acyl group formation was suppressed because *ac*cA inhibition disrupted FAS. Fewer acyl groups negatively affect lipid bilayers and the biofilm of bacterial cells.

LuxS produces AI-2, and AI-2 signaling molecules monitor metabolism, assist with forming a biofilm, allows the transport of metabolite molecules, and transports regulatory signals [36]. Jia et al. found the growth and metabolism of the *luxS* mutant knockout strain decreased because the reduction of fatty acid metabolic synthesis degraded cell membrane fluidity [39]. Inhibiting *accA* produced an incomplete fatty acid elongation cycle that suppressed *luxS* because the availability of FAs and acyl groups decreased and lowered the fluidity of the cell membrane. Gram-negative bacterial transmembrane proteins are implanted in the hydrophobic interior of lipid bilayers, and FAS of lipids and phospholipids affect the composition of the cell membrane [4]. The viscosity (thickness) or fluidity of the lipid bilayer is significant for the activity of membrane proteins. Membrane lipid bilayer thickness changes as the membrane fluidity and phases are altered for allocating proteins to different regions and phases of the bacterial cell membrane [40]. The varied configurations of lipids control the physicochemical properties of the cell membrane such as viscosity, rigidity, phase behavior, and membrane fluidity [41, 59]. Unsaturated lipids have a double bond that creates a kink in lipids that prevents tight lipid packing in the cell membrane and increase fluidity.

High membrane fluidity permits a facile diffusion and rotation of membrane proteins. Membrane fluidity is defined as the ease in which lipids and proteins can diffuse across the cell membrane. The acyl chain compositions in the cell membrane lipids largely determine membrane fluidity. Disrupting FASII via *accA* inhibition can form lipid bilayers with altered lipid composition that reduce membrane fluidity needed for the LsrACDB transmembrane protein to operate. Disrupting FAS causes less cell membrane fluidity, and then lessens the diffusion of transmembrane proteins in the lipid bilayer. A LsrACDB transmembrane protein in a rigid lipid bilayer cannot move easily in the hydrophobic regions, delaying the influx of AI-2. Less intracellular AI-2 blocks its phosphorylation by LsrK, required to initiate the LuxS/AI-2 QS system. Less internal AI-2 may have downregulated *luxS* gene expression after inhibiting accA, blocked FASII, and lowered membrane fluidity.

Hence, a higher awareness of the interaction between bacterial metabolic potency and virulence is needed [42]. According to Stokes et al., we are currently at the beginning stages of understanding the link between bacterial metabolism and antibiotic efficacy [43]. Pisithkul et al. demonstrated that the growth of biofilm temporally was suppressed in the absence of viable nutrients within the interior of *B. subtilis* cells [8]. Zuberi et al. applied CRISPRi technology to inhibit *luxS* genes in *E. coli* cells and found that biofilm formation depended upon the expression of *luxS*. Zuberi et al. used a crystal violet test to assess the effect of *luxS* on biofilm. Biofilm formation decreased as *luxS* expression was reduced [45]. In a rat model, the LuxS/AI-2 quorum-sensing system of *S. pneumoniae* is required for biofilm formation to spread to the ear epithelium, resulting in an ear infection. LuxS/AI-2 controls expression of genes specific for affecting virulence and bacterial fitness as the biofilm of *S. pneumoniae* forms [60].

Many pathogens express LuxS [44] where LuxS regulates bacterial metabolism and conducts frequent quorum sense events. To connect bacterial metabolism with the virulence of biofilm, this study attempted to integrate bacterial FAS with *luxS* activity by inhibiting the catalysis of FASII, then analyzing the luxS response. The activity of the LuxS/AI-2 QS system*, which* assists with forming biofilm*,* is linked to carbohydrate metabolism because by increasing glucose increments, Wang et al. found that glucose intensified the levels of AI-2 in culture [30]. Added glucose amplifies FASII, the FAs increase membrane fluidity, and mediate AI-2 proliferation, which upregulates *luxS*. This study attempted to reveal this bacterial metabolic to virulence link when eliminating FASII via inhibition of *accA*, decreasing the fluidity that caused less influx of AI-2. Less internal AI-2 then downregulated *luxS*. The research findings of this study advocate for the further identification and elucidation of more bacterial metabolic to virulence links.

Figure 12 *accA* affects *luxS* expression, *accA* exhibits a proportional relation with *luxS*.

A) As *accA* expression decreased during asRNA inhibition, *luxS* expression reduced in tandem.

B) **The heat map shows** decreased *accA* (Dark Purple) values yielded higher Cp values for *luxS* (Neon Yellow). The highest Cp value of 20 was produced at position 13 for a Log_{accA} value approximately near 0. Less *luxS* DNA present is indicative of a higher CP value for *luxS* at a decreased *accA* expression level. C) Displays a logarithmic relation between *luxS* and log_{accA} that as *accA* approaches 0, the expression of *luxS* decreases. When *accA* reaches a threshold, *luxS* peaks, but then *luxS* reaches equilibrium as *accA* increases. D) The Cp Values for *luxS* were parallel and matched in a majority of log_{accA} data replicates. E) The QQ plot shows the means are normally distributed for *luxS,* Cp values, and log_{accA}. F) The sigmoidal plot shows a cooperative relation between accA and luxS.

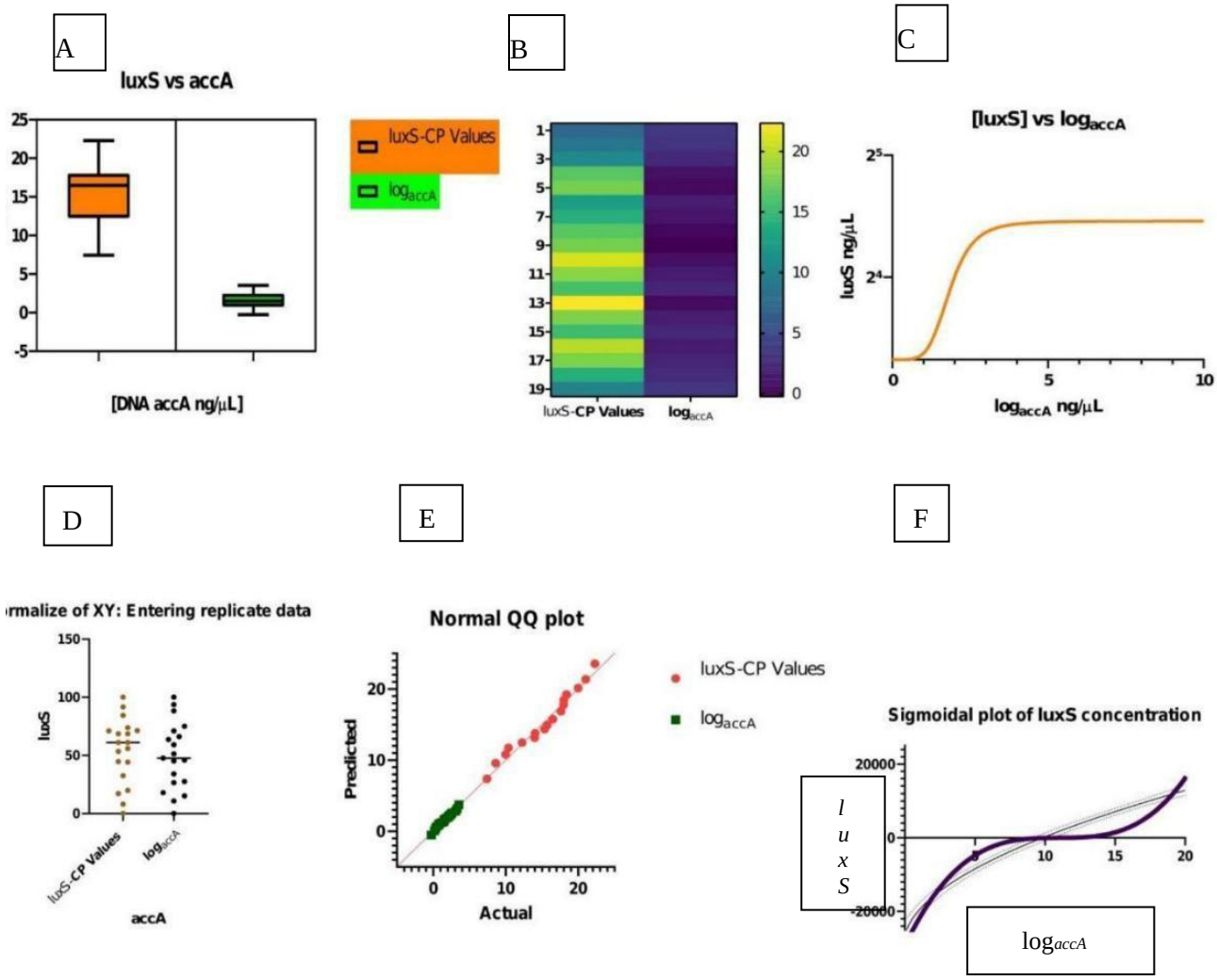

ANTIBIOTIC RESISTANCE TEST

An antibiotic resistance test was performed to determine the susceptibility of antibiotics from *E. coli* sample cultures expressing antisense RNA inhibition of the gene *accA.* The bacterial samples showing pHN1257-asRNA-*accA* gene suppression were predominantly susceptible to the antibiotic's tetracycline (10µg/mL), carbenicillin (100µg/mL), and chloramphenicol (25µg/mL) (Fig 13). Disks (N=64) consisting of each of the three antibiotics were placed on agar plates divided into eight sections. The zone of inhibition was measured in millimeters. For the experimental group (with asRNA), the median was 20 mm for the measurement of the zone of inhibition. The control group (without (+)asRNA-accA) were mainly resistant to antibiotics, with an average of 6 mm ZOI. Bacteria transformed with pHN1257-(+)asRNA-*accA* were more susceptible to the antibiotic's tetracycline, carbenicillin, and chloramphenicol (Fig 14).

Fifty-nine percent of the experimental (+)asRNA-*accA* samples were sensitive to tetracycline, chloramphenicol, and carbenicillin (21±4, SEM=0.7). The (+)asRNA- *accA* treatment group displayed an intermediate sensitivity of 28% as 3% (95% CI, [6, 20]) were resistant to antibiotics (13.75±10, SEM=1.8). The control exhibited more resistance with 25%, 12.5%, and 53% of susceptibility, intermediate, and resistance, respectively. The (+) asRNA-*accA* treatment group had an 82% (95% CI, [6, 20]) difference in sensitivity compared to the (-)asRNA-*accA* control group. The control group showed 77% (95% CI, [6, 20]) variation in resistance when compared to the (+)asRNA-*accA* experimental group (p=0.000554). A paired t-test was performed, yielding a t-score of 3.6, and degrees of freedom equaling 31. The t-score and DF were used to calculate the p-value ($p<0.05$).

The antibiotic susceptibility of gram-negative *E. coli* can rise because inhibiting *accA* to disrupt FASII breaks down the lipid bilayer of its IM (inner membrane). An incomplete PM of IM can permit an elevated influx of antibiotics into the cytoplasm of previously drug-resistant *E. coli*. The antisense inhibition of *accA* disrupted fatty acid synthesis and elongation. Less access to viable fatty acids such as the acyl-ACPs led to an unstable plasma membrane structure for the *E. coli* cells. The incomplete plasma membrane then allowed the facile transport of the antibiotics, chloramphenicol, tetracycline, and carbenicillin to cross the double membrane of the gram-negative *E. coli* bacterial cells, which lowered its antibiotic resistance. The bacterium of *S. aureus* translates a lysine at its 164th genomic locus, forming an *S. aureus* that is resistant to the antibiotic called thailandamide. The thaillandamide also denatures and deactivates the AccA transferase subunit. The bacterium of *Salmonellae* also produces a mutation in the gene for *accA*. Other antibiotics, such as capistruin and malleilactone, are novel synthetic antibiotics that inhibit the transformation process between bacterial cells. This blockage of bacterial transformation causes increased production of antibiotics [46]. However, wild-type *S. aureus* incorporates exogenous and dissimilar fatty acids into its PM at significant phospholipid positions without the need for FASII antibiotic selection and this may cancel the previously assumed explanation for fatty acid selectivity of phospholipid synthesizing enzymes [47].

In contrast, FASII antibiotic adaptation involves robust bacterial proliferation and incorporation of host fatty acids. Bacterial metabolism and environmental stress play concrete roles in the outcome of antimicrobial treatments [47]. Such metabolic fortitude allows bacteria to salvage metabolites from their environment. This consideration may limit the potential of selected ACCs as metabolic targets for antimicrobial drug development. Exogenous fatty acids are converted into acyl-ACP in some gram-negative bacteria. The resulting acyl-ACP undergoes the same fate as endogenously synthesized acyl-ACP. Exogenous fatty acids are converted into acyl-phosphate in gram-positive bacteria and can be used for phospholipid synthesis or converted into acyl-ACP. Only *Lactobacillales* can use exogenous fatty acids to bypass FASII inhibition [48]. FASII shuts down entirely in the presence of exogenous fatty acids in *Lactobacillales*, allowing *Lactobacillales* to synthesize phospholipids entirely from exogenous fatty acids. Inhibition of FASII cannot be bypassed in other bacteria because FASII is only partially downregulated in the presence of exogenous fatty acids or FASII is required to synthesize essential metabolites such as β-hydroxyacyl-ACP [48].

The difference between mammalian and bacterial ACCase enzymes is vital for designing single-target antibiotics and antimicrobial gene knockout mutations of *accA*. An antibiotic designed to inhibit a bacterial ACCase enzyme cannot interfere or interact with a mammalian ACCase enzyme because the mammalian ACC isoforms differ from the bacterial ACCs. Mammals have a different isoform of ACC called ACC2 or ACCβ. ACCβ is conserved and matches 73% of its amino acids with the identity of isoforms ACC1 and ACC2 from humans [16]. ACC2 in mammals' functions as an enzyme located in the outer membrane of the mitochondria. ACC2 maintains a 140-residue orientation at the N-terminus. This 140-residue of amino acids located near the N-terminus is not present in the bacterial ACC [16]. The preceding 20 side chain residues of the 140 residues were almost wholly hydrophobic.

ACCase enzymes found in eukaryotes differ from those used by prokaryotes. In eukaryotic cells, BC has three domains, the A, B, and C domains. The side chain residue groups of A and C contain the active site. The domain of B enormously changes its conformation to cover the active site during the reaction. Eukaryotic cells have a BC domain with many partitioned and segmented residues. The side chain residues measure 550 residues between the BC and AB connecting domains as compared to bacterial BC units that contain 450 residues [16]. The subunits of the ACCase enzyme complex are favorable targets for antibiotic design because the bacterial ACCs are immensely different from mammalian and human ACC isoforms. Inhibiting bacterial ACCs cannot negatively modify or interfere with mammalian and human ACCase enzymes.

FIGURE 13 Zone of inhibition and Antibiotic Susceptibility Test

Bacteria that were transformed with pHN1257-(+)asRNA-*accA* showed greater susceptibility to the antibiotic disk containing tetracycline, chloramphenicol, and carbenicillin. Twenty-seven of the total 64 samples were susceptible to antibiotics. Eighteen of the samples were resistant, and 13 were only intermediate. The ratio of (+)asRNA-*accA* to (-)asRNA-*accA* equaled 3:2. B) Within the range of 20 to 22 mm of ZOI for the (+) asRNA-*accA* expressing bacteria, the antibiotic susceptibility showed a density of 0.01515. The control displayed less susceptibility at 20 to 30 mm ZOI with a density of 0.007.

A)

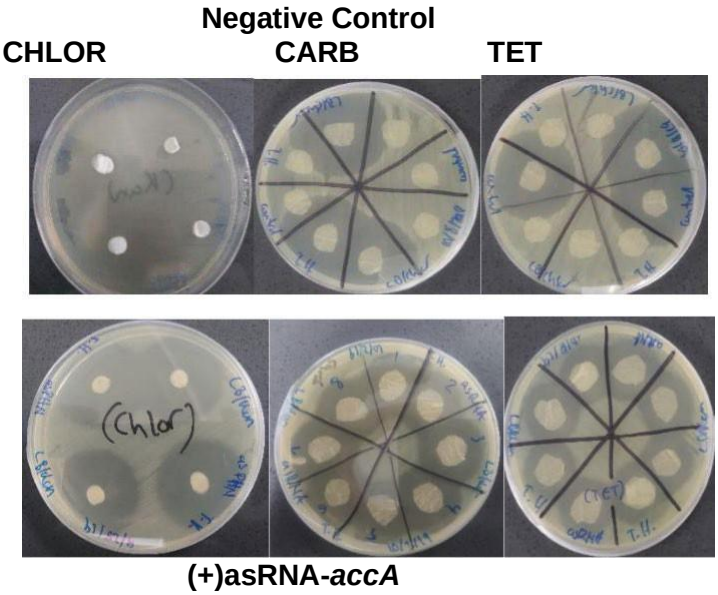

(+)asRNA-*accA*

B)

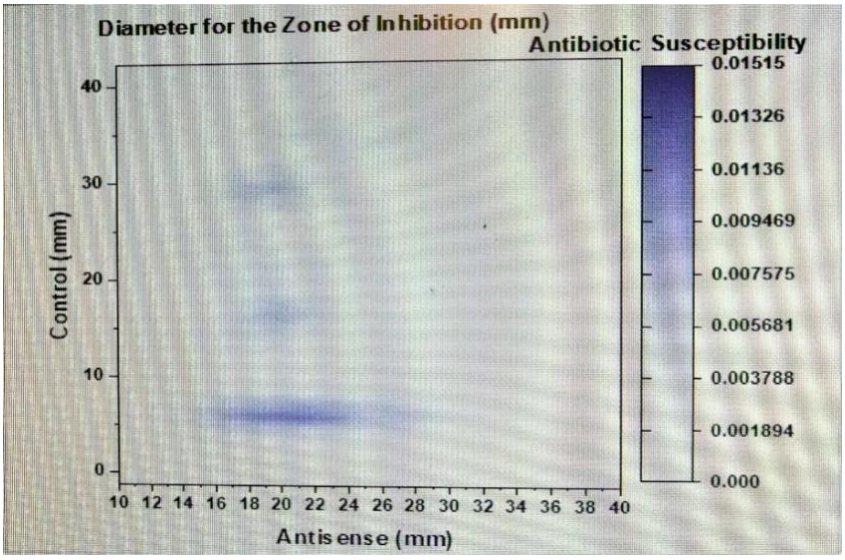

Figure 14 Zone of Inhibition A) There was a 60% (95% CI, [6, 20]) percent difference in the span of ZOI between the *accA*-mutant knockout and the control. The *accA* gene mutant showed a higher level of ZOI. B) The QQ plot exhibited a normal distribution of data residuals for the *accA*-mutant and the control. C) The heat map displays the control with a dominant green color and the *accA*- mutant produced darker hues as a black color. The green color for the control is an indicator of a lower level of ZOI and the darker hue as the red and black of the *accA*-mutant specifies an elevated distance of ZOI. D) The homoscedasticity of residual data points is not maintained and is nonlinear. E) The observed ZOI residual data points were different from the predicted ZOI for the *accA*-mutant and the control, demonstrating a nonlinear regression.

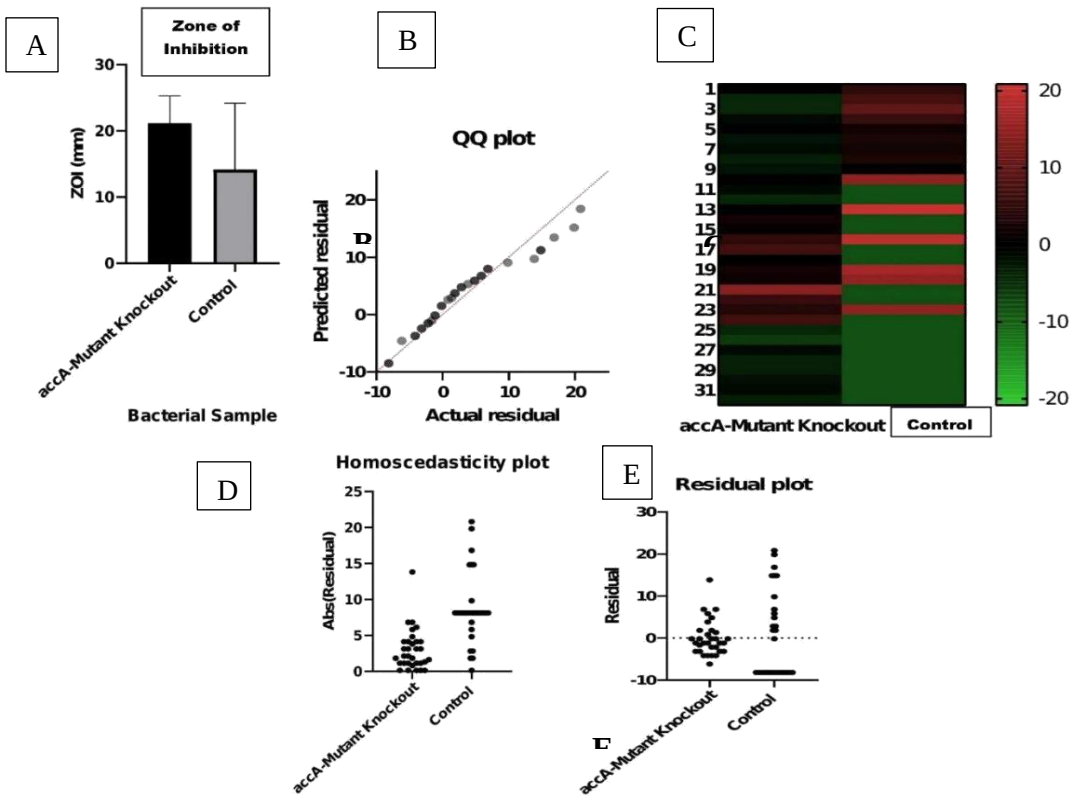

CONCLUSION

Multidrug-resistant Gram-negative bacteria (MDR-GNB) have created an intense challenge for clinicians in treating infections of ill patients in intensive care units [49]. Higher rate of MDR-GNB are partially attributed to the double membrane of Gram-negative bacteria. The Gram-negative bacteria cell wall differs more than Gram-positive bacteria. Gram-negative bacteria have a cell envelope that contains an outer membrane consisting of LPS with endotoxins, a peptidoglycan cell wall, and an inner membrane. Gram-positive bacteria do not incorporate an outer membrane. The outer membrane can restrict the penetration of antibiotics into Gram-negative bacteria cells [50]. Only in current years has GNB become resistant to all common categories of antimicrobials [49].

The resistance of novel antibiotics has begun to rise and administering these novel antibiotics has been limited to decrease any further occurrence of MDR. Recently, most drug companies have developed novel antimicrobials that have focused on Gram-positive bacteria. Many new and novel antibiotics have not been produced to combat Gram-negative bacteria [51]. The issue of MDR-resistant gram-negative bacteria and less new antibiotics to act against these MDR-GNBs has forced the administration of old antibiotics such as polymyxin B and polymyxin E. The polymyxins combat gram-negative bacteria such as Pseudomonas aeruginosa and *Enterobacter* species [52]. Antimicrobial peptides (AMPs) can degrade the bacterial structure by directly interacting with the membranes of microbes through electrostatic activity [53]. However, many AMPs have not achieved success in clinical studies because they are extremely toxic for mammalian cells.

Antimicrobial gene therapies may provide more novel antimicrobials for increasing antibiotic susceptibility of MDR gram-negative bacteria. The accA gene may represent a potential target for novel antimicrobial gene therapy. Because the DNA of the ACCase enzyme is conserved across many different species, targeting it with novel antibiotic-gene inhibition can eradicate the function and presence of the ACCase protein. Conserved DNA sequences do not mutate or change. If the DNA of the conserved sequence for the ACCase enzyme is inhibited or altered, then the enzyme will lack expression and completely lose its function.

This study presented important results for the effect of glucose and the inhibition of *accA* on *luxS*, an essential component of bacterial biofilm formation, quorum sense signaling, and virulence. accA encodes the AccA subunit of CT, which catalyzes FASII. Inhibiting accA did decrease luxS gene expression. Suppression of luxS after silencing accA occurred because inhibiting *accA* lessened fatty acid production that decreased cell membrane fluidity. Disrupting quorum sense signaling was exhibited in the reduction of *luxS* after silencing accA. The expression of *luxS* is an essential factor of virulence. The qPCR absolute quantification results determined the total sum of gene copies for *luxS* decreased during *accA inhibition*. *E. coli* (+)asRNA-*accA* cell cultures produced 199 gene copies of luxS versus the control. The control yielded $1x10^6$ gene copies for luxS. Suppressing luxS can prevent biofilm formation and disrupt the LuxS/AI-2 QS system. Preventing biofilm creation and reducing QS activity can lessen the virulence of pathogenic bacteria. Bacteria that are highly virulent need to use biofilm for binding to epithelial cells and then spread infection.

The accumulation of AI-2 is used by bacteria to infect more host cells, and AI-2 creates a more solid biofilm [48]. The activity of the flagella is amplified with higher levels of *luxS* mutations present in the lungs and bloodstream. The mutant *luxS* allows bacteria to infect the lungs and blood more than the wild-type strain [49]. LuxS produces the DPD precursor for AI-2 synthesis [44]. The purpose of LuxS and AI-2 includes regulating metabolism and monitoring quorum sense activity [44]. The LuxS protein plays a significant role for generating infections [44]. The *luxS* gene, when it is more expressed, causes the spread of virulent bacteria by increasing the motility of pathogenic bacteria.

When Lux-S and AI-2 are less regulated and overexpressed, infectious bacteria can propagate in stressful environments with high acidity and salinity [54]. Kendall et al. (2008) demonstrated the ability of *S. pyogenes* to adapt to acidic conditions because of an upregulated Lux-S/AI-2 system [55]. The mutation of *luxS* in *Haemophilus influenzae* increases virulence and then causes middle ear infections [49]. The many facets of biofilm to tolerate antimicrobial therapy include many different types and subtypes of metabolic actions that regulate the bacterial response to different metabolic stimuli. The subtypes of metabolic changes include responses to pH, osmotic pressure, and the availability of nutrients [26].

The overall purpose of this study was to link bacterial metabolism such as the ACCase AccA-CT enzymatic catalysis of FASII with LuxS/AI-2 dependent virulence. The potent metabolic state of a bacterial population can inhibit bacterial susceptibility of antibiotics [56], therefore, suppressing bacterial metabolism may increase antibiotic sensitivity. E. coli cells expressing (+)asRNA-*accA* showed more susceptibility of antibiotics because asRNA blocked *accA* translation into AccA, which eliminated the AccA subunit from the ACCase-CT enzyme. A CT without AccA subunits cannot bind to carboxyls to catalyze FASII. Less FASII degrades the IM of gram-negative bacteria, and a damaged IM allows a more facile influx of hydrophilic antibiotics. However, there are limitations of this study where hydrophilic antibiotics could not be added to cell cultures during antibiotic susceptibility tests. If hydrophilic antibiotics were used, a more distinguished ZOI and percent difference between the experimental and control could have been shown. Hydrophilic antibiotics were not available at the time, but the antibiotic tests still exhibited higher rates of susceptibility for (+)-asRNA-*accA* cell cultures.

There is a significant link between bacterial cell metabolism and virulence. The metabolism of carbohydrates controls biofilm generation in many bacterial species [37]. For example, it was found that increased glucose availability allowed *S. epidermidis* to upregulate transcription specific for biofilm production during the stationary growth phase [62]. However, other bacteria from the *Enterobacteriaceae* species suppress the creation of biofilm with heightened glucose. Many other gram-positive bacteria also repress biofilm formation in the presence of glucose. In bacterial species, *E. faecalis* augments its genesis of biofilm when glucose is in excess, but many different strains of *E. faecalis* can

also repress biofilm construction while glucose is present [38]. The biofilm contains the total biomass of a bacterial community. The availability of nutrients determines the amount of biomass that accumulates within a biofilm. Adding glucose supplementation to the culture medium increases bacterial growth and total biomass of a biofilm [34].

Understanding the metabolic dependency of bacterial virulence may become fundamental for designing novel antibiotics. During the past 30 years, the formulation and discovery of potent antibiotics have dwindled [57], and there is a gap in the literature concerning the connection between bacterial metabolism and virulence. However, there exists an immense possibility to design novel antibiotics that target bacterial metabolic genes through genetic engineering of antimicrobials. Future research could design multiple novel antibiotics by identifying and targeting metabolic gene targets with antibiotic gene therapy. Hall et al. concluded that the cause of antibiotic resistance or antibiotic sensitivity of biofilm originates from a genetic source [58]; therefore, perhaps combating MDR-GNB requires a gene-based antimicrobial approach. Hopefully, this study's attempt to describe the interaction between fatty acid metabolism and virulence may add to our understanding of metabolic-dependent pathogenesis in Gram-negative bacteria.

ACKNOWLEDGMENTS Special thanks are given to the staff from TheLAB in Los Angeles, CA. Thank you for your team. They were always available for answering questions and providing support.

Funding: The author received no specific funding for this work.
Conflicts of interest: The authors declare no conflicts of interest.

REFERENCES

1.Eichenberger EM, Thaden JT. Epidemiology and Mechanisms of Resistance of Extensively Drug Resistant Gram-Negative Bacteria. Antibiotics. 2019 Jun;8(2):37.

2.Richie, D. L., Wang, L., Chan, H., De Pascale, G., Six, D. A., Wei, J. R., & Dean, C. R. (2018). A pathway-directed growth restoration assay to facilitate the discovery of lipid A and fatty acid biosynthesis inhibitors in Acinetobacter baumannii. *PloS one*, *13*(3).

3.Epand RM, Walker C, Epand RF, Magarvey NA. Molecular mechanisms of membrane targeting antibiotics. Biochimica et Biophysica Acta (BBA)-Biomembranes. 2016 May 1;1858(5):980-7.

4.Silhavy TJ, Kahne D, Walker S. The bacterial cell envelope. Cold Spring Harbor perspectives in biology. 2010 May 1;2(5):a000414.

5.Konovalova A, Silhavy TJ. Outer membrane lipoprotein biogenesis: Lol is not the end. Philosophical Transactions of the Royal Society B: Biological Sciences. 2015 Oct 5;370(1679):20150030.

6.Sweeney, P., Murphy, C. D., & Caffrey, P. (2016). Exploiting the genome sequence of Streptomyces nodosus for enhanced antibiotic production. *Applied microbiology and biotechnology*, *100*(3), 1285-1295

7.Broussard, T. C., Kobe, M. J., Pakhomova, S., Neau, D. B., Price, A. E., Champion, T. S., & Waldrop, G. L. (2013). The three-dimensional structure of the biotin carboxylase-biotin carboxyl carrier protein complex of E. coli acetyl-CoA carboxylase. *Structure*, *21*(4), 650-657.

8.Pisithkul, T., Schroeder, J. W., Trujillo, E. A., Yeesin, P., Stevenson, D. M., Chaiamarit, T., ... & Amador-Noguez, D. (2019). Metabolic remodeling during biofilm development of Bacillus subtilis. *MBio*, *10*(3), e00623-19.

9.Yao, J., & Rock, C. O. (2017). Exogenous fatty acid metabolism in bacteria. Biochimie, 141, 30-39.

10.Dubois-Brissonnet, F., Trotier, E., & Briandet, R. (2016). The biofilm lifestyle involves an increase in bacterial membrane saturated fatty acids. *Frontiers in microbiology*, *7*, 1673.

11.N. Nakashima, T. Tamura. Conditional gene silencing of multiple genes with antisense RNAs and generation of a mutator strain of Escherichia coli. Nucleic Acids Res. 2009;103 (37).

12.Joyce EA, Kawale A, Censini S, Kim CC, Covacci A, Falkow S. LuxS is required for persistent pneumococcal carriage and expression of virulence and biosynthesis genes. Infection and Immunity. 2004 May 1;72(5):2964-75.

13.Jia, F. F., Pang, X. H., Zhu, D. Q., Zhu, Z. T., Sun, S. R., & Meng, X. C. (2017). Role of the luxS gene in bacteriocin biosynthesis by Lactobacillus plantarum KLDS1. 0391: A proteomic analysis. *Scientific reports*, *7*(1), 1-14.

14.Milke, L., Kallscheuer, N., Kappelmann, J., & Marienhagen, J. (2019). Tailoring Corynebacterium glutamicum towards increased malonyl-CoA availability for efficient synthesis of the plant pentaketide noreugenin. *Microbial cell factories*, *18*(1), 71.

15.Waldrop, G. L.; Rayment, I.; Holden, H. M. (1994). "Three-dimensional structure of the biotin carboxylase subunit of acetyl-CoA carboxylase". Biochemistry. **33** (34): 10249– 10256. *doi*:*10.1021/bi00200a004*. *PMID* 7915138.

16.Tong, L. (2013). Structure and function of biotin-dependent carboxylases. *Cellular and Molecular Life Sciences*, *70*(5), 863-891.

17.Lietzan, A. D., & Maurice, M. S. (2013). A substrate-induced biotin binding pocket in the carboxyltransferase domain of pyruvate carboxylase. *Journal of Biological Chemistry*, *288*(27), 19915-19925.

18.Seti, Gita. (n.d). Discover Ideas about Protein. Retrieved from https://www.pinterest.com/pin/531002612291400564/ on June 30, 2020

19.Chandrakar, B., Jain, A., Roy, S., Gutlapalli, V. R., Saraf, S., Suppahia, A., ... & Nayarisseri, A. (2013). Molecular modeling of Acetyl-CoA carboxylase (ACC) from Jatropha curcas and virtual screening for identification of inhibitors. *journal of pharmacy research*, *6*(9), 913-918.

20.Bilder P, Lightle S, Bainbridge G, Ohren J, Finzel B, Sun F, Holley S, Al-Kassim L, Spessard C, Melnick M, Newcomer M, Waldrop GL. The structure of the carboxyltransferase component of acetyl-coA carboxylase reveals a zinc-binding motif unique to the bacterial enzyme. *Biochemistry* **45** 1712-22 (2006) doi:10.1021/bi0520479

21.Broussard, T. C., Price, A. E., Laborde, S. M., & Waldrop, G. L. (2013). Complex formation and regulation of Escherichia coli acetyl-CoA carboxylase. *Biochemistry*, *52*(19), 3346-3357.

22.Ikeda, M., Nagashima, T., Nakamura, E., Kato, R., Ohshita, M., Hayashi, M., & Takeno. (2017). In vivo roles of fatty acid biosynthesis enzymes in biosynthesis of biotin and α-lipoic acid in Corynebacterium glutamicum. *Appl. Environ. Microbiol.*, *83*(19), e01322-17.

23.Salie, M. J., Zhang, N., Lancikova, V., Xu, D., & Thelen, J. J. (2016). A family of negative regulators targets the committed step of de novo fatty acid biosynthesis. *The Plant Cell*, *28*(9), 2312-2325.

24.Evans, A. L. (2018). The Distinctive Regulatory Mechanisms of Bacterial Acetyl- CoA Carboxylase.

25.Janiyani, K., Bordelon, T., Waldrop, G. L., & Cronan, J. E. (2001). Function of Escherichia coli biotin carboxylase requires catalytic activity of both subunits of the homodimer. Journal of Biological Chemistry, 276(32), 29864-29870.

26.Dubois-Brissonnet, F., Trotier, E., & Briandet, R. (2016). The biofilm lifestyle involves an increase in bacterial membrane saturated fatty acids. *Frontiers in microbiology*, *7*, 1673.

27.France, M. T., Cornea, A., Kehlet-Delgado, H., & Forney, L. J. (2019). Spatial structure facilitates the accumulation and persistence of antibiotic-resistant mutants in biofilms. *Evolutionary Applications*,

12(3), 498-507.

28.Rojo-Molinero, E., Macià, M. D., & Oliver, A. (2019). Social behavior of antibiotic-resistant mutants within Pseudomonas aeruginosa biofilm communities. *Frontiers in Microbiology*, *10*, 570.

29.Trappetti, C., Potter, A.J., Paton, A.W., Oggioni, M.R. and Paton, J.C. LuxS mediates iron-dependent biofilm formation, competence, and fratricide in Streptococcus pneumoniae. Infection and Immunity. 2011;79(11):4550-4558.

30.Wang, L., Hashimoto, Y., Tsao, C.Y., Valdes, J.J. and Bentley, W.E. Cyclic AMP (cAMP) and cAMP receptor protein influence both synthesis and uptake of extracellular autoinducer 2 in Escherichia coli. Journal of bacteriology. 2005;187(6):2066-2076.

31.Jesudhasan, P.R., Cepeda, M.L., Widmer, K., Dowd, S.E., Soni, K.A., Hume, M.E., Zhu, and Pillai, S.D. Transcriptome analysis of genes controlled by *luxS*/autoinducer-2 in Salmonella Enterica serovar Typhimurium. Foodborne pathogens and disease.2010;7(4):399-410.

32.C.M. Waters, B.L. Bassler. Quorum sensing: cell-to-cell communication in bacteria. Annu. Rev. Cell Dev. Biol. 2005;21: 319-346.

33.S.T. Freestone, B.L. Bassler. Bacterial Quorum Sensing: Its Role in Virulence and Possibilities for Its Control. Cold Spring Harbor Perspectives in Medicine. 2012;2(11): a012427. doi:10.1101/cshperspect. a012427.

34.Pillai, S. K., Sakoulas, G., Eliopoulos, G. M., Moellering Jr, R. C., Murray, B. E., & Inouye, R. T. (2004). Effects of glucose on fsr-mediated biofilm formation in Enterococcus faecalis. *Journal of Infectious Diseases*, *190*(5), 967-970.

35.Li, J., Attila, C., Wang, L., Wood, T. K., Valdes, J. J., & Bentley, W. E. (2007). Quorum sensing in Escherichia coli is signaled by AI-2/LsrR: effects on small RNA and biofilm architecture. *Journal of bacteriology*, *189*(16), 6011-6020.

36.Widmer, K. W., Jesudhasan, P., & Pillai, S. D. (2012). Fatty acid modulation of autoinducer (AI-2) influenced the growth and macrophage invasion by Salmonella Typhimurium. *Foodborne pathogens and disease*, *9*(3), 211-217.

37.Nicol, M., Alexandre, S., Luizet, J. B., Skogman, M., Jouenne, T., Salcedo, S. P., & Dé,
E. (2018). Unsaturated Fatty Acids Affect Quorum Sensing

Communication System and Inhibit Motility and Biofilm Formation of Acinetobacter baumannii. *International journal of molecular sciences*, *19*(1), 214. https://doi.org/10.3390/ijms19010214

38.Schaefer, A., Greenberg, E., Oliver, C. *et al.* A new class of homoserine lactone quorum- sensing signals. *Nature* **454,** 595–599 (2008). https://doi.org/10.1038/nature07088

39.Jia, F. F., Pang, X. H., Zhu, D. Q., Zhu, Z. T., Sun, S. R., & Meng, X. C. (2017). Role of the luxS gene in bacteriocin biosynthesis by Lactobacillus plantarum KLDS1. 0391: A proteomic analysis. *Scientific reports*, *7*(1), 1-14.

40. Gorhbandt M, Lipski A, Baig Z, Walter S, Kurre R, Strahl H, Deckers-Hebestreit G. Low membrane fluidity triggers lipid phase separation and protein segregation in vivo. BioRxiv. 2019 Jan 1:852160.

41.Ballweg S, Ernst R. Control of membrane fluidity: the OLE pathway in focus. Biological Chemistry. 2017 Feb 1;398(2):215-28.

42.Stokes, J. M., Lopatkin, A. J., Lobritz, M. A., & Collins, J. J. (2019). Bacterial metabolism and antibiotic efficacy. *Cell metabolism*.

43.Baquero F, Martínez JL. Interventions on metabolism: making antibiotic- susceptible bacteria. mBio. 2017 Dec 29;8(6):e01950-17.

44.Zuberi A, Misba L, Khan AU. CRISPR interference (CRISPRi) inhibition of luxS gene expression in E. coli: an approach to inhibit biofilm. *Frontiers in cellular and infection microbiology.* 2017 May *26;***7***:*214*.*

45.Vendeville, A., Winzer, K., Heurlier, K., Tang, C.M., and Hardie, K.R., Making' sense of metabolism: autoinducer-2, LuxS, and pathogenic bacteria. Nature Reviews Microbiology. 2005;3(5):383.

46.Kénanian, G., Morvan, C., Weckel, A., Pathania, A., Anba-Mondoloni, J., Halpern, D., & Poyart, C. (2019). Permissive Fatty Acid Incorporation Promotes Staphylococcal Adaptation to FASII Antibiotics in Host Environments. Cell Reports, 29(12), 3974-3982.

47.Passalacqua, K. D., Charbonneau, M. E., & O'riordan, M. X. (2016). Bacterial metabolism shapes the host-pathogen interface. *Virulence Mechanisms of Bacterial Pathogens*, 15-41.

48.Yao, J., & Rock, C. O. (2017). Exogenous fatty acid metabolism in bacteria. Biochimie, 141, 30-39

49.Bassetti M, Peghin M, Vena A, Giacobbe DR. Treatment of infections due to MDR Gram-negative bacteria. Frontiers in medicine. 2019 Apr 16;6:74.

50.Exner M, Bhattacharya S, Christiansen B, Gebel J, Goroncy-Bermes P, Hartemann P, Heeg P, Ilschner C, Kramer A, Larson E, Merkens W. Antibiotic resistance: What is so special about multidrug-resistant Gram-negative bacteria?. GMS hygiene and infection control. 2017;12

51.Giamarellou H. Multidrug-resistant Gram-negative bacteria: how to treat and for how long. International Journal of Antimicrobial Agents. 2010 Dec 1;36:S50-4.

52.Falagas ME, Kasiakou SK, Saravolatz LD. Colistin: the revival of polymyxins for the management of multidrug-resistant gram-negative bacterial infections. Clinical infectious diseases. 2005 May 1;40(9):1333-41.

53.Lam SJ, O'Brien-Simpson NM, Pantarat N, Sulistio A, Wong EH, Chen YY, Lenzo JC, Holden JA, Blencowe A, Reynolds EC, Qiao GG. Combating multidrug-resistant Gram-negative bacteria with structurally nanoengineered antimicrobial peptide polymers. Nature microbiology. 2016 Sep 12;1(11):1-1.

54.M.M. Kendall, D.A. Rasko, V. Sperandio. Global effects of the cell-to-cell signaling molecule autoinducer-2, autoinducer-3, and epinephrine in a *luxS* mutant of enterohemorrhagic Escherichia coli." Infection and Immunity. 2007;75(10):4875-4884.

55.Vidal, J.E., Ludwick, H.P., Kunkel, R.M., Zahner, ¨ D. and Klugman, K.P. The LuxS dependent quorum-sensing system regulates early biofilm formation by Streptococcus pneumoniae strainD39. Infection and immunity. 2011;79(10):4050-4060.

56.Ludwick, H.P., Nava, P., and Klugman, K.P., 2013. Quorum-sensing systems LuxS/autoinducer two and Com regulate Streptococcus pneumoniae biofilms in a bioreactor with living cultures of human respiratory cells. Infection and immunity. 2013;81(4): 1341-1353.

57.Polyak SW, Abell AD, Wilce MC, Zhang L, Booker GW. Structure, function, and selective inhibition of bacterial acetyl-CoA carboxylase. Applied microbiology and biotechnology. 2012 Feb 1;93(3):983-92.

58.Hall CW, Mah TF. Molecular mechanisms of biofilm-based antibiotic resistance and tolerance in pathogenic bacteria. *FEMS microbiology reviews.* 2017 Mar *25;***41***(*3*):*276–301.

59. Ballweg S, Sezgin E, Doktorova M, Covino R, Reinhard J, Wunnicke D, Hänelt I, Levental I, Hummer G, Ernst R. Regulation of lipid saturation without sensing membrane fluidity. Nature communications. 2020 Feb 6;11(1):1-3.

60. Yadav MK, Vidal JE, Go YY, Kim SH, Chae SW, Song JJ. The LuxS/AI-2 quorum-sensing system of Streptococcus pneumoniae is required to cause disease, and to regulate virulence-and metabolism-related genes in a rat model of middle ear infection. Frontiers in cellular and infection microbiology. 2018 May 4;8:138.

61.Soares, A., Caron, F., & Etienne, M. (2019). Commentary: tolerance and resistance of pseudomonas aeruginosa biofilms to antimicrobial agents–how p. Aeruginosa can escape antibiotics. *Frontiers in Microbiology*, *10*, 2164.

62.Dobinsky, S., Kiel, K., Rohde, H., Bartscht, K., Knobloch, J. K. M., Horstkotte, M. A., & Mack, D. (2003). Glucose-related dissociation between icaADBC transcription and biofilm expression by Staphylococcus epidermidis: evidence for an additional factor required for polysaccharide intercellular adhesin synthesis. *Journal of bacteriology*, *185*(9), 2879-2886.